CORROSION CHARACTERISTICS OF ALUMINIUM ALLOYS IN CALOPHYLLUM INOPHYLLUM BIODIESEL

RAJA NURUL HANI BINTI RAJA AZHAR

FACULTY OF ENGINEERING
UNIVERSITY OF MALAYA
KUALA LUMPUR

2017

CORROSION CHARACTERISTICS OF ALUMINIUM ALLOYS IN CALOPHYLLUM INOPHYLLUM BIODIESEL

RAJA NURUL HANI BINTI RAJA AZHAR

RESEARCH REPORT SUBMITTED IN PARTIAL FULFILMENT OF THE REQUIREMENTS FOR THE DEGREE OF MASTER OF MECHANICAL ENGINEERING

FACULTY OF ENGINEERING
UNIVERSITY OF MALAYA
KUALA LUMPUR

2017

UNIVERSITY OF MALAYA

ORIGINAL LITERARY WORK DECLARATION

Name of Candidate: **Raja Nurul Hani Binti Raja Azhar**

(I.C/Passport No:

Registration/Matric No: **KQK 160009**

Name of Degree: **Masters of Mechanical Engineering**

Title of Project Paper/Research Report/Dissertation/Thesis ("this Work"):

Corrosion Characteristics of Aluminium Alloys in Calophyllum Inophyllum Biodiesel

Field of Study: **Corrosion**

I do solemnly and sincerely declare that:

(1) I am the sole author/writer of this Work;
(2) This Work is original;
(3) Any use of any work in which copyright exists was done by way of fair dealing and for permitted purposes and any excerpt or extract from, or reference to or reproduction of any copyright work has been disclosed expressly and sufficiently and the title of the Work and its authorship have been acknowledged in this Work;
(4) I do not have any actual knowledge nor do I ought reasonably to know that the making of this work constitutes an infringement of any copyright work;
(5) I hereby assign all and every rights in the copyright to this Work to the University of Malaya ("UM"), who henceforth shall be owner of the copyright in this Work and that any reproduction or use in any form or by any means whatsoever is prohibited without the written consent of UM having been first had and obtained;
(6) I am fully aware that if in the course of making this Work I have infringed any copyright whether intentionally or otherwise, I may be subject to legal action or any other action as may be determined by UM.

Candidate's Signature Date:

Subscribed and solemnly declared before,

Witness's Signature Date:

Name:

Designation:

CORROSION CHARACTERISTICS OF ALUMINIUM ALLOYS IN CALOPHYLLUM INOPHYLLUM BIODIESEL

ABSTRACT

Biodiesel is one of the attractive alternatives to cater the limited petroleum diesel sources in future due to its environmental benefit and domestic producibility. However, one of the drawbacks of biodiesel is its corrosive property. In this work, corrosion characteristics of commercial aluminium alloy 3003, 5052 and 6061 in various Calophyllum inophyllum biodiesel blends is studied and analyzed. Immersion test of aluminium alloy 3003, 5052 and 6061 is carried out in Calophyllum inophyllum biodiesel blends B0, B5, B10 and B15 for 1200 hours at room temperature. The corrosion rate of aluminium alloy 3003, 5052 and 6061 in Calophyllum inophyllum biodiesel blends B0, B5, B10 and B15 is calculated from the weight loss obtained after the immersion test. The surface morphology after immersion test is observed by using scanning electron microscopy (SEM). Result shows that aluminium alloy 3003 is the most susceptible to corrosion in Calophyllum inophyllum biodiesel blends compared to aluminium alloy 5052 and 6061.

Keywords: corrosion, aluminium, biodiesel.

PENGARATAN ALOI ALUMINIUM DALAM CALOPHYLLUM INOPHYLLUM BIODIESEL

ABSTRAK

Biodiesel merupakan salah satu alternatif yang menarik untuk menampung sumber diesel petroleum yang terhad pada masa depan berikutan manfaat alam sekitar dan keluaran domestiknya. Walau bagaimanapun, salah satu kelemahan biodiesel adalah sifatnya yang menghakis. Dalam penyelidikan ini, ciri-ciri kehakisan aloi aluminium komersial 3003, 5052 dan 6061 dalam pelbagai campuran Calophyllum inophyllum biodiesel dikaji dan dianalisis. Ujian rendaman aloi aluminium 3003, 5052 dan 6061 dilakukan dalam campuran B0, B5, B10 dan B15 Calophyllum inophyllum biodiesel selama 1200 jam pada suhu bilik. Kadar karat aloi aluminium 3003, 5052 dan 6061 dalam campuran B0, B5, B10 dan B15 Calophyllum inophyllum biodiesel dikira daripada perbezaan berat selepas ujian rendaman. Morfologi permukaan selepas ujian rendaman diperhatikan dengan menggunakan mikroskop elektron pengimbas (SEM). Keputusan menunjukkan bahawa aloi aluminium 3003 adalah yang paling mudah terdedah kepada karat dalam campuran Calophyllum inophyllum biodiesel berbanding aloi aluminium 5052 dan 6061.

Kata kunci: karat, aluminium, biodiesel.

ACKNOWLEDGEMENTS

I am grateful to Allah, The Almighty for His Countless Blessings and giving me strength, opportunity and knowledge to persevere the challenges and obstacles in the accomplishment of this research project.

First and foremost, I would like to use this opportunity to express my earnest gratitude and appreciation to my respected supervisor, Dr. Nazatul Liana binti Sukiman for her endless support and guidance to complete this research project successfully within the time frame. Without her support, this research project would not have been possible.

Next, special thanks to Miss Nor Wahida Subri for providing her heartfelt support and invaluable guidance throughout the completion of this research project. I am grateful to receive her unconditionally assistance at all time.

I also would like to thank Mr. Premdass A/L Deva Ray, Mr. Vikneswaran A/L Padasivam and Mr. Mohd Ashraf Mohd Yusoff for their assistance and support in completing this research project.

Last but not least, I would like express my deep gratitude for my beloved family and friends for their unconditionally love, support, motivation, inspiration and blessings throughout thick and thin. Without their unwavering support and love, this achievement may not have been possible.

TABLE OF CONTENTS

CORROSION CHARACTERISTICS OF ALUMINIUM ALLOYS IN CALOPHYLLUM INOPHYLLUM BIODIESEL ABSTRACT iii

PENGARATAN ALOI ALUMINIUM DALAM CALOPHYLLUM INOPHYLLUM biodiesel ABSTRAK iv

ACKNOWLEDGEMENTS v

LIST OF FIGURES viii

LIST OF TABLES x

LIST OF SYMBOLS AND ABBREVIATIONS xi

CHAPTER 1: INTRODUCTION 1

- 1.1 Overview 1
- 1.2 Problem Statement 3
- 1.3 Objectives 4
- 1.4 Scope of Study 4

CHAPTER 2: LITERATURE REVIEW 5

- 2.1 Overview 5
- 2.2 The Basic of Corrosion 5
- 2.3 Faraday’s Law in Corrosion Study 6
- 2.4 Corrosion in Aluminium Alloy 10
  - 2.4.1 Aluminium Alloy 10
  - 2.4.2 Corrosion Mechanism in Aluminium Alloy 15
- 2.5 Corrosion in Biodiesel 23
  - 2.5.1 Biodiesel Production 23
  - 2.5.2 Calophyllum Inophyllum Biodiesel 28
  - 2.5.3 Corrosion Mechanism in Biodiesel 34
- 2.6 Corrosion Characterization Technique 39
  - 2.6.1 Weight Loss Analysis 39

CHAPTER 3: METHODOLOGY 41

- 3.1 Overview 41
- 3.2 Biodiesel Blends Preparation 43
- 3.3 Sample Preparation 46

3.4 Immersion Test 48
3.4.1 Post Immersion Sample Cleaning 50
3.4.2 Data Collection and Analysis 51
3.5 Surface Characterization 52
3.5.1 Scanning Electron Microscope (SEM) 52
CHAPTER 4: RESULTS AND DISCUSSION 53
4.1 Overview 53
4.2 Immersion Test 53
4.3 Surface Characterization 59
4.3.1 Sample Before Immersion Test 59
4.3.2 Immersion in B0 61
4.3.3 Immersion in Calophyllum Inophyllum Biodiesel Blend B15 63
CHAPTER 5: CONCLUSION 67
REFERENCE 69
APPENDIX A 76

LIST OF FIGURES

Figure 2.1: Arrangement of local-action cells at metal surface (Revie, 2008). 7
Figure 2.2 : Mechanism of corrosion behavior in aluminium (Ostermann & Woodward, 1993).. 15
Figure 2.3 : : Pourbaix diagram shows the corrosion potential of aluminium with oxide film immersed in various pH of aqueous solution at 25 ^{o}C (E. A. Association, 2002) 16
Figure 2.4 : Principle alloying element effect on the corrosion potential of aluminium alloy in electrolytic solution (J. R. Davis, 1999).. 18
Figure 2.5 : Surface image of pitting corrosion on pure aluminium surface (Pereira, Silva, Acciari, Codaro, & Hein, 2012) 19
Figure 2.6 : Pitting corrosion process 20
Figure 2.7 : Cross section image of pitting corrosion on pure aluminium surface (Pereira et al., 2012).. 21
Figure 2.8 : Chemical reaction during transesterification process (Alenezi, Baig, Wang, Santos, & Leeke, 2010) 25
Figure 2.9 : Flow chat of transesterification process in biodiesel production (Mofijur et al., 2016).. 25
Figure 2.10 : Three common FAME molecular structures in biodiesel. 28
Figure 2.11 : Calophyllum inophyllum tree grows on sand (Friday & Okano, 2006)......... 29
Figure 2.12 : Calophyllum inophyllum fragrant white flowers that flowering heaviest in the late spring and early summer (Friday & Okano, 2006).. 29
Figure 2.13 : Nearly matured fruit of Calophyllum inophyllum (Friday & Okano, 2006).. 30
Figure 2.14 : Dried seeds of Calophyllum inophyllum (Atabani & da Silva César, 2014) . 31
Figure 2.15 : Separation of dried kernel from shell of dried Clophyllum inophyllum seeds (Atabani & da Silva César, 2014) 31
Figure 2.16 : Process involves in Calphyllum inophyllum biodiesel production (Ashok et al., 2017).. 32
Figure 2.17 : Three stages involved in the oxidation of biodiesel (Zuleta et al., 2012)....... 34
Figure 3.1 : Procedure of static immersion test technique for corrosion study.................. 41
Figure 3.2 : Calophyllum inophyllum biodiesel B100 obtained from University of Malaya. 44
Figure 3.3 : Calophyllum inophyllum biodiesel blend is stirred using magnetic stirrer Fisher Scientific Isotemp Heated Magnetic Stirrer / Hotplate 45
Figure 3.4 : Three Calophyllum inophyllum biodiesel blends, B5 (left), B10 (middle) and B15 (right) 45
Figure 3.5 : Aluminium alloy sample (1 inch x 1 inch) for static immersion test. 47
Figure 3.6 : Aluminium alloy sample is weighed using Sartorius Digital Weighing Scale. 48
Figure 3.7 : Aluminium alloy samples immersed in various Calophyllum inophyllum biodiesel blends 49
Figure 3.8 : Ultrasonic cleaner used to clean the sample after immersion test. 50
Figure 3.9 : PHENOM ProX table top SEM available in University of Malaya 52

Figure 4.1 : Corrosion rate of aluminium alloys after immersion in Calophyllum inophyllum biodiesel blends at room temperature for 1200h. 54
Figure 4.2: BSE-SEM image before immersion test at 1000X... 59
Figure 4.3: BSE-SEM image before immersion test at 4500X... 60
Figure 4.4: BSE-SEM image after immersion test in B0 at 1000X 61
Figure 4.5: BSE-SEM image after immersion test in B0 at 4500X 62
Figure 4.6: BSE-SEM image after immersion test in B15 at 1000X 63
Figure 4.7: BSE-SEM image after immersion test in B15 at 4500X 64

LIST OF TABLES

Table 2.1 : Aluminium wrought alloy series and principal alloying elements (J. Davis, 1994)........ 12
Table 2.2 : Various potential feedstock for biodiesel around the world (Mahmudul et al., 2017)........ 24
Table 2.3 : Comparison the properties of fuel of biodiesel B100, B6 to B20 and Diesel based on ASTM D6751, ASTM D7467 and ASTM D975 respectively (Testing & Materials, 2010). 26
Table 2.4 : Properties of Calophyllum inphyllum biodiesel developed by Atabani et al. (Atabani et al., 2013)........ 33
Table 2.5: Fatty acid composition of Calophyllum inophyllum biodiesel (Jahirul et al., 2014)........ 33
Table 2.6: Corrosion rate unit based on constant K value. (Metals, 2011)........ 40
Table 3.1 : Fuel properties of Calophyllum inophyllum biodiesel (Ong, Mahlia, Masjuki, & Norhasyima, 2011)........ 43
Table 3.2: Kinetic viscosity, dynamic viscosity and density of Calophyllum inophyllum biodiesel blends........ 44
Table 3.3 : Chemical composition of aluminium alloy 3003, 5052 and 6061 (A. Association, 2009)........ 46
Table 4.1: Average weight loss and corrosion rate of the samples........ 54

LIST OF SYMBOLS AND ABBREVIATIONS

Al : Aluminium
Al^{3+} : Aluminium ion
Al_2O_2 : Dialuminium dioxide
Al_2O_3 : Aluminium oxide
ANSI : Americans National Standards Institute
ASTM : American Society for Testing and Materials
B0 : Commercial diesel
B5 : 5 percent Calophyllum inophyllum biodiesel blend
B10 : 10 percent Calophyllum inophyllum biodiesel blend
B15 : 15 percent Calophyllum inophyllum biodiesel blend
B100 : Pure Calophyllum inophyllum biodiesel
BSE : Back-scattered electrons
C : Carbon
Cl^- : Chloride
CO : Carbon monoxide
CO_2 : Carbon dioxide
Cr : Chromium
Cu : Copper
FAME : Fatty acid methyl ester
Fe : Iron
H^+ : Hydrogen ion
H_2 : Hydrogen

H_2O : Water
KOH : Potassium hydroxide
Mg : Magnesium
Mg_2Si : Magnesium silicide
Mn : Manganese
NaCl : Sodium chloride
NaOH : Sodium hydroxide
Ni : Nickel
O_2 : Oxygen
OH^- : Hydroxyl ion
SEM : Scanning electron microscopy
Si : Silicon
SiO_2 : Silicon dioxide
Ti : Titanium
Zn : Zinc

LIST OF APPENDICES

Appendix A: Weight measurement data for AA 3003, AA 5052 and AA 6061 before and after immersion test in Calophyllum inophyllum biodiesel blends B0, B5, B10 and B15 for 1200 hours at room temperature.. 76

CHAPTER 1: INTRODUCTION

1.1 Overview

Transportation plays an important role to the development of economy in many countries. In United States, Bureau of Transportation Statistic reported there is 399% increase and 507% increase on the transportation demand and Gross Domestic Products (GDP) respectively from 1980 to 2014 (Moore, 2005). The report clearly shows that the transportation demand increases as the economy keeps growing. As the transportation demand increase, the fuel demand will be also increases. Based on BP Statistical Review of World Energy 2016, it is observed that the world oil consumption increases by 12.14% from year 2005 to 2015 (Dudley, 2016). The increasing on the petroleum demand over the years will cause a shortage in petroleum supply in future since petroleum is non-renewable resources.

One of the alternatives to cope with increasing demands for fuel in transportation sector is by producing biodiesel. The first application of vegetable oil in diesel engine has been demonstrated by Rudolph Diesel at Paris Exposition in 1900 (Nitske & Wilson, 1965). Later, the vegetable oils were also used in the emergency situation during the period of World War II in 1940’s as one of the diesel engine fuel (F. Ma & Hanna, 1999). After the petroleum crisis in 1980’s, large scale worldwide production of biodiesel increases tremendously between 1980 and 2005 where European Union, United States, Argentina, Brazil, Australia, Malaysia, Indonesia, India and Canada are some of the countries that actively producing biodiesel (Armbruster & Coyle, 2006; Murray, 2005; OECD & FAO, 2009). The use of edible oil as biodiesel feedstock can cause the competition between food and fuel sources demand that lead to food price crisis in year 2007 to 2008 (Owen, Inderwildi, & King, 2010; Rosegrant, 2008). In order to solve this problem, more non-edible biodiesel has been introduced. Calophyllum inophyllum oil is one of the non-edible biodiesel produced from the dried seed of Calophyllum inophyllum tree that mostly populated in India, Southeast Asia and Australia (Atabani & da Silva César, 2014). The advantages of Calophyllum inophyllum biodiesel are it has high oil yield, better lubrication capability and high heating value (Sudradjat, 2011).

However, some studies showed that biodiesel is more corrosive compared to petroleum diesel (Fazal, Haseeb, & Masjuki, 2010; Haseeb, Masjuki, Ann, & Fazal, 2010; Hu, Xu, Hu, Pan, & Jiang, 2012; Jin, Zhou, Wu, Jiang, & Ge, 2015; Kaul et al., 2007; Singh, Korstad, & Sharma, 2012; Su, Chen, Wu, & Wang, 2014; Thangavelu, Ahmed, & Ani, 2016). Corrosion can cause metal degradation, thus reduce the mechanical strength that may lead to material failure in the long run. Aluminium alloys is one of the material used to make fuel tank due to its high strength to weight ratio and good corrosion resistance properties (Miller et al., 2000). The corrosion of fuel tank can cause oil to leak, so the frequent placement of vehicle fuel tank is required that increase the maintenance expenditure. So far, there is no research has been done to study the possibility of Calophyllum inophyllum biodiesel causing corrosion in aluminium alloys. Therefore, by conducting a study of "Corrosion characteristics of aluminium alloys in Calophyllum inophyllum biodiesel," it is hoped that the phenomena of corrosion that involves aluminium alloy parts and Calophyllum Inophyllum biodiesel can be understood, hence provide the necessary information towards the application of Calophyllum Inophyllum biodiesel in diesel fuel system in future.

1.2 Problem Statement

Biodiesel is one of the renewable resources that have been introduced as an alternative to reduce the dependency on the petroleum diesel. The production of biofuel increases by 14.1% from year 2005 to 2015 due its compatibility to the existing diesel engine system and other advantages such as low greenhouse gas emission, improve fuel lubricity, biodegradable and non-toxic (Dudley, 2017). Despite of the numerous advantages, the drawback of biodiesel is its corrosive property.

Corrosion is a natural phenomenon that can cause material deterioration due to chemical or electrochemical reaction between the material and its environment. Corrosive property of biodiesel can damage the automotive components, hence reduces the life time of the parts. Researches stated that the biodiesel has corrosive behavior due to free water and fatty acids contents in biodiesel (Fazal et al., 2010; Haseeb, Masjuki, et al., 2010). Haseeb et al. stated that different types of fatty acids can be produced from the oxidation of biodiesel, hence it is more corrosive compared to as-received biodiesel (Haseeb, Masjuki, et al., 2010).

In Malaysia, palm oil is the main feedstock in biodiesel production and cooking oil. In order to reduce the dependency on palm oil (since palm oil is also the main source of food in Malaysia), Calophyllum inophyllum biodiesel is one of the suitable candidates that can replace palm oil biodiesel since it is non-edible and abundantly available feedstock in Malaysia. However, there is no study have been done on the corrosive property of Calophyllum inophyllum biodiesel. From this study, the corrosion behavior of Calophyllum inophyllum can be studied and analyzed.

1.3 Objectives

In order to study the corrosion characteristics of aluminium alloys in Calophyllum inophyllum biodiesel, some objectives have been set in this project.

a) To identify the corrosion rate of aluminium alloy 3003, 5052 and 6061 in Calophyllum inophyllum biodiesel at room temperature.

b) To study the corrosion morphology of aluminium alloy 3003, 5052 and 6061 in Calophyllum inophyllum biodiesel at room temperature.

c) To investigate the effect of Calophyllum inophyllum biodiesel blends B5, B10 and B15 on the corrosion rate of aluminium alloys at room temperature.

1.4 Scope of Study

The scope of this project is to study the corrosion behavior of aluminium alloy 3003, 5052 and 6061 by immersion test in Calophyllum inophyllum biodiesel blends B5, B10 and B15 at room temperature for 1200 hours exposure time. The corrosion rate of different combination of aluminium alloy and Calophyllum inopyllum blends are identified by measuring the weight loss after the static immersion test. SEM is used to analyze the corrosion morphology of aluminium alloys.

CHAPTER 2: LITERATURE REVIEW

2.1 Overview

This chapter explains the definition of corrosion and theoretical Faraday's Law in corrosion study. Next, the commercial aluminium alloys is introduced and the mechanism of corrosion in aluminium alloy is explained briefly. The common pitting corrosion behavior of aluminium is also explained in this chapter. After that, biodiesel production in general and corrosion mechanism in biodiesel are explained briefly. Calophyllum inophyllum biodiesel is also introduced. Finally, the mass loss analysis technique used to study the corrosion rate is explained briefly.

2.2 The Basic of Corrosion

Corrosion is a process where the material such as metal, polymer and etc. is degraded due to the interaction between the surface of material and the environment. Union of Pure and Applied Chemistry (IUPAC) (2012) define corrosion as below:

> An irreversible interfacial reaction of a material (metal, ceramic, polymer) with its enviroment which results in consumption of the material or in dissolution into the material of a component of the enviroment. Often, but not necessarily, corrosion results in effects detrimental to the usage of the material considered. Exclusively physical or mechanical processes such as melting or evaporation, abrasion or mechanical fracture are not included in the term corrosion. (p.340).

In another perspective, Ahmad (2006) defines corrosion into four definitions which are shown below:

A. Corrosion is the surface wastage that occurs when metals are exposed to reactive environments.
B. Corrosion is the results of interaction between the metal and environments with results in its gradual destruction.
C. Corrosion is an aspect of the decay of the materials by chemical or biological agents.
D. Corrosion is an extractive metallurgy in reverse.

(Ahmad, 2006, p. 2)

In conclusion, corrosion can be defined as a natural irreversible process where the materials react to the environment and produce a chemical compound (usually to the nature state of compound) that can cause damage to the materials. Corrosion is considered as defect to the material because it can cause deterioration to the affected material. In order to prevent corrosion, a lot of studies have been done to understand the corrosion phenomena so that the preventive measures can be developed to protect the material from corrosion.

2.3 Faraday's Law in Corrosion Study

In the early nineteenth century, Michael Faraday carried out a quantitative electrochemical reaction experiment and developed Faraday's Law which states that the mass discharged at electrode is directly proportional to the electrical charged flow through the electrode. (Kelly, Scully, Shoesmith, & Buchheit, 2002). Faraday also identified the charge that one mole of electrons carries one Faraday, F which equals to 96,485 Coulombs, C will oxide or reduce one gram of material during electrochemical reaction. In corrosion study, the corrosion rate can be determined by using the same principle as Faraday's Law.

At any surface of material, the electrodes are electrically short circuited within the material itself which is known as local-action cells (Figure 2.1) (Revie, 2008) . The local-action cells cannot be detected on the dry material (without electrolyte exposure), however when the metal is exposed to electrolytic solution, the local-action cells reacts to the solution where the regions are divided into positive charged (anode) and negative charged region (cathode), allow the electrons to flow within the cells, thus allow the corrosion to take place on the surface of the material.

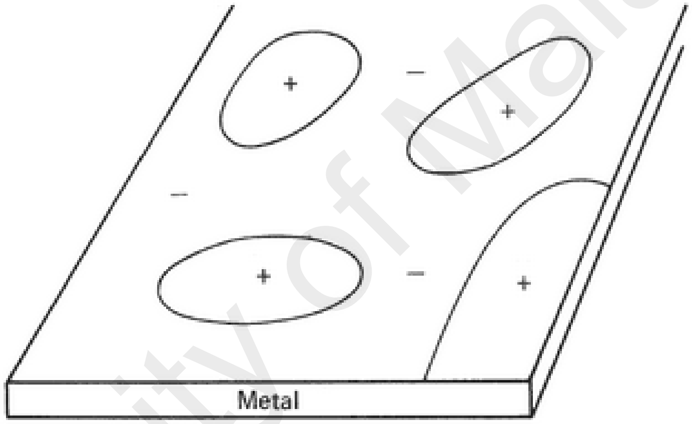

Figure 2.1: Arrangement of local-action cells at metal surface (Revie, 2008).

During corrosion, the electrons moves from anode region to cathode region within the metal itself at certain rate that can be measured as anodic current, I_{cor}. From the assumption that the current is uniform across the surface area, the corrosion current density, i_{cor} is calculated by dividing anodic current, I_{cor} by the surface area exposed to the corrosive environment, A (Equation 2.1).

$$\boldsymbol{i_{corr} = \frac{I_{corr}}{A}} \tag{2.1}$$

Where i_{corr} is corrosion current density in μA/cm^2, I_{corr} is anodic current in μA and A is surface area exposed to corrosive environment in cm^2. Corrosion current density indicates the rate of electron flow per unit area of surface during corrosion process. The higher the corrosion current density, the faster the electron moves from anode to cathode per unit area, thus the faster the oxidation process occurs at anode.

Material loss rate from corrosion process at anode can be determined by measuring the anodic current. The relationship between the mass loss and electric current is shown by using Faraday's law (Equation 2.2).

$$\boldsymbol{m = \frac{I\,t\,M}{n\,F}} \tag{2.2}$$

Where m is weight loss in grams, I is electric current in Ampere, t is time in second, M is molar mass in gram per mole, F is Faraday constant and n is the number of valence electrons of material. Corrosion rate can be determined by dividing the (Equation 2.2) by time, t and surface area, A (Equation 2.3).

$$\boldsymbol{r = \frac{i_{corr}\,M}{n\,F}} \tag{2.3}$$

Where r is corrosion rate and i_{corr} is corrosion current density in μA/cm^2. This shows that the corrosion rate is directly proportional to the corrosion current density. In design, penetrating rate in mil per year (mpy) is more useful (Equation 2.4).

$$\boldsymbol{mpy = \frac{129\,(M)(i_{corr})}{n\,\rho}} \tag{2.4}$$

Where mpy is penetration rate in mils per year, M is atomic mass in gram, i_{corr} is the corrosion current density in mA/cm^2, ρ is density in g/cm^3 and n is the number of valence electron. Equation 2.4 is appropriate equation to calculate the corrosion rate of the pure material. In alloy material, a few elements contain various valence electrons are bonded together, so the corrosion rate calculated in Equation 2.4 is not accurate for alloy. To identify the corrosion rate of alloy, the atomic weight and valence electrons of each element in the alloy must be considered in the calculation. For a unit mass oxidized where the electron equivalent to 1 gram of alloy is oxidized, the charge Q is calculated in Equation 2.5.

$$\boldsymbol{Q = \sum \frac{n_i f_i}{W_i}} \qquad \textbf{(2.5)}$$

Where n_i is the valence electron of the i^{th} element of the alloy, f_i is the mass fraction of i^{th} element in the alloy and W_i is the atomic weight of element i^{th} in the alloy. The equivalent weight loss of alloy during corrosion process can be determined from Equation 2.6.

$$\boldsymbol{w = \frac{1}{\sum \frac{n_i f_i}{W_i}}} \qquad \textbf{(2.6)}$$

For the calculation in Equation 2.5 and 2.6, only the elements that is greater than one percent in the alloy composition involve in the calculation.

2.4 Corrosion in Aluminium Alloy

2.4.1 Aluminium Alloy

Aluminium alloy has been used widely in various applications such as aeronautic, transportation, building and construction, electrical, marine application, beverage containers and etc. due to its nature properties that can fulfill the application requirements. Some advantages of aluminium alloy are lightweight, good electrical and thermal conductor, high resistant to corrosion, high strength, durable and malleable. Aluminium alloy is also suitable to make fuel storage tank due to its high resistant to corrosion property.

In nature, aluminium is found in a compound form mixed with silicon and oxygen known as bauxite, usually mined in the rock minerals region. Aluminium is soft, lightweight, non-magnetic and has dull silvery appearance. The atomic number of aluminium is 13 and it is highly reactive metal. In 1855, the first commercial aluminium was produced by H. Sainte-Claire Deville in France (Downs, 1993). The extraction of aluminium involves two major stages which are purification of raw material stage and reduction of alumina stage.

In purification of raw material stage, bauxite are crushed and washed to remove the impurities. Next, the remained material is dissolved in sodium hydroxide and heated. During the reaction, the aluminiujm oxide and silicon dioxide are dissolved in sodium hydroxide and produce sodium hexahydroxoaluminate, $Na_3Al(OH)_6$ (Equation 2.7). Over a period of time, the sodium hexahydroxoaluminate, $Na_3Al(OH)_6$ decomposes to aluminium hydroxide, $Al(OH)_3$. Then, the heating of aluminium hydroxide to above $1000^{o}C$ decomposes the material to alumina, Al_2O_3.

$$Al_2O_3 + 6\,NaOH + 3H_2O \rightarrow 2Na_3\,Al(OH)_6 \tag{2.7}$$

$$SiO_2 + 4NaOH \rightarrow Na_4SiO_4 + 2H_2O \tag{2.8}$$

In reduction of alumina stage, the alumina is dissolved in molten cryolite, Na_3AlF_6. This reaction produces electrically conductive solution, thus allow the extraction process to be done by electrolysis method by using carbon anode with two concurrent reactions (Equation 2.9-2.10). Then, the aluminium is ready to mix with the other alloying elements.

$$Al_2O_3 + 3C \rightarrow 2Al + 3CO \tag{2.9}$$

$$2Al_2O_3 + 3C \rightarrow 4Al + 3CO_2 \tag{2.10}$$

Pure aluminium has the capability to produce oxide layer on its surface to protect the surface layer from reaction, hence has the high resistant to corrosion. Besides, the pure aluminium is also a good electrical conductor and good formability. However, pure aluminium is very soft and not able to withstand the high load. Due to low strength in pure aluminium, the other elements are added to produce aluminium alloy to improve the strength in aluminium while maintaining the good properties of aluminium. The greatest advantage of aluminium alloy is the aluminium alloy has high strength to density ratio, so it is very suitable to use to make strong lightweight structure.

Some alloying elements that are commonly used for alloying the aluminium are copper, manganese, silicon, magnesium and zinc. Aluminium alloy is classified according to the standard in Aluminium Association Alloyand Temper Designation System recognized by ANSI. There two grading systems in aluminium alloy based on the alloy fabrication namely wrought alloy and cast alloy.

Aluminium wrought alloy is classified into a few series denoted by four-digit numerical system (xxxx). The first digit indicates the the principal alloying element in aluminium, the second digit indicates the variation of initial alloy while the third and fourth digit indicates the arbitrary number in the series. The principal alloy elements for different alloy series is shown in Table 2.1. Different principal alloying element contribute different feature to the aluminum series.

Table 2.1 : Aluminium wrought alloy series and principal alloying elements (J. Davis, 1994).

Aluminium Series	Principal Alloying Element
1xxx	99% Al and above
2xxx	Copper
3xxx	Manganese
4xxx	Silicon
5xxx	Magnesium
6xxx	Magnesium and Silicon
7xxx	Zinc
8xxx	Other Elements

Aluminium alloy 1xxx series has the highest aluminium content in its alloy, so the properties of aluminium alloy 1xxx series is almost similar to the pure aluminium. Aluminium alloy 1xxx is commonly used in electrical and chemical applications due to its high electrical and thermal conductivity and high corrosion resistance. However, aluminium alloy 1xxx series is very soft, so it is not suitable for the application that requires high strength and toughness.

Aluminium alloy 2xxx series is composed of copper as the principal alloying element and often added magnesium as the secondary element. Aluminium alloy 2xxx requires heat treatment to improve its mechanical properties such as strength. Aluminium alloy 2xxx series is commonly used to make structures that requires high strength to weight ratio such as aircraft application and truck suspension. However, the disadvantage of aluminium alloy 2xxx series is susceptible to intergranular corrosion and has the lowest corrosion resistance compared to the other aluminium alloy.

In aluminium alloy 3xxx series, manganese is the principal alloying element. The addition of manganese increases the alloy strength while maintaining the ductile property of aluminium. Aluminium alloy 3xxx series is commonly used in general purpose application that requires moderate strength and good workability such as roof sheet and canning industry.

Aluminium alloy 4xxx series has the lowest melting point due to the addition of silicon in its alloy. Aluminium alloy 4xxx is suitable for the application that requires low melting point such as welding wire and brazing alloy for aluminium joint, commonly used in architectural industry. Aluminium 4xxx series also ha low thermal coefficient and high wear resistance that is suitable for production forged engine pistons.

Aluminium alloy 5xxx is made by the addition of magnesium as its principal alloying element in its alloy. Aluminium alloy 5xxx series has good weldability and corrosion resistance in marine condition. Due to these properties, aluminium alloy 5xxx series is suitable for the marine applications. However, the content of magnesium must not exceed 3% to avoid the stress corrosion cracking.

Aluminium alloy 6xxx series contains silicon and magnesium as its principal alloying elements. Aluminium alloy 6xxx series has god formability, good corrosion resistance, good weldability and good machinability. Aluminium alloy 6xxx series is commonly used in transportation, building and structure application. However, the silicon and magnesium content must not exceed the required amount to produce magnesium silicide to avoid intergranular corrosion.

Aluminium alloy 7xxx series is composed of highest percentage of zinc that act as principal alloying element, with small percentage of magnesium and copper. Aluminium alloy 7xxx has the highest strength compared to the other aluminium alloys. Aluminium alloy 7xxx series is commonly used in aircraft and military vehicle application due to its high tensile strength property. However, the high strength of aluminium alloy 7xxx reduce the corrosion resistance.

Aluminium alloy 8xxx series composed of various chemical compositions without having specific pattern. The properties of aluminium alloy 8xxx series depends on the element content in its alloy. For instance, Al-Fe-Ce alloys can improve the performance at elevated temperature.

2.4.2 Corrosion Mechanism in Aluminium Alloy

Aluminium is a very reactive metal, but at the same time become a passive metal when it comes to corrosive environment. Aluminium forms a thin oxide layer on the surface. In general, during the corrosion process, when the thin layer is damaged, aluminium quickly reforms the thin oxide layer and continues to prevent the surface from reacting to the environment. In severe corrosive environment, the oxide film is damaged severely and cannot repaired, then the aluminium surface will have a direct contact to the environment and the corrosion process will take place.

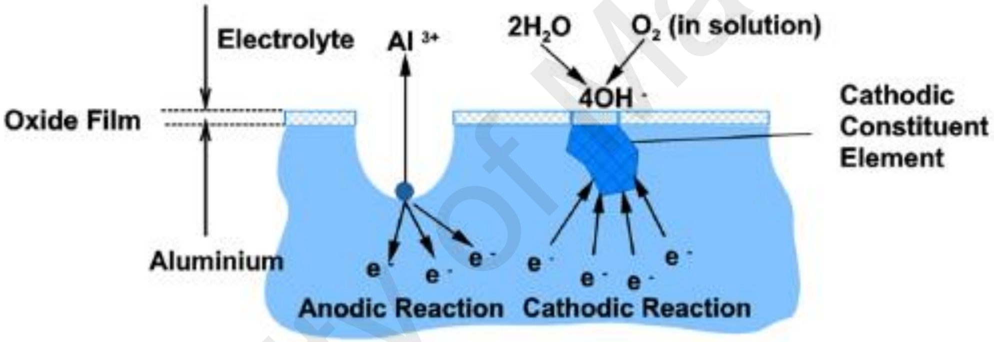

Figure 2.2 : Mechanism of corrosion behavior in aluminium (Ostermann & Woodward, 1993)

The corrosion behavior of aluminium alloy is highly dependent on the stability of protective oxide layer. Acidity level and alkalinity level of the electrolyte affect the stability of protective oxide layer of aluminium (Zaid, Saidi, Benzaid, & Hadji, 2008). The relationship between pH and potential, V is represented by Pourbaix diagram (Figure 2.3). There are three corrosion behaviors of aluminum in electrolyte; corrode, show immunity and passivate (E. A. Association, 2002).

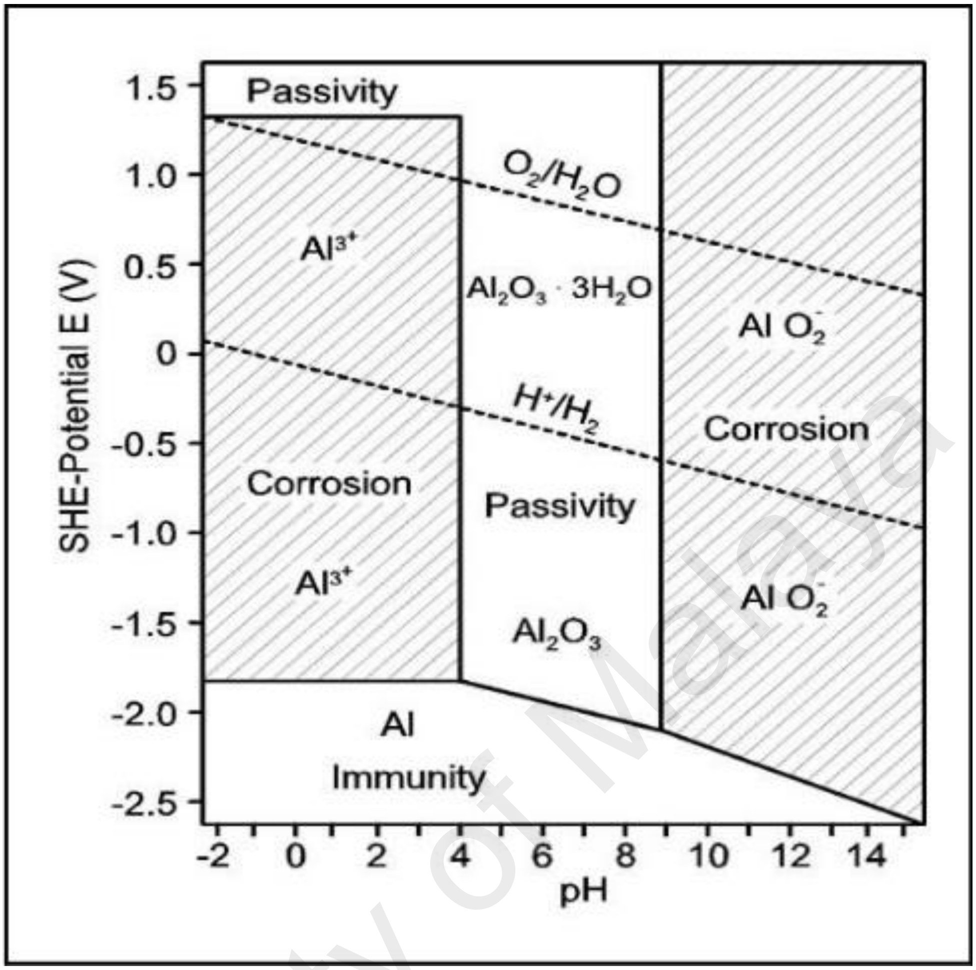

Figure 2.3 : : Pourbaix diagram shows the corrosion potential of aluminium with oxide film immersed in various pH of aqueous solution at 25 ^{o}C (E. A. Association, 2002)

Aluminium corrodes in acidic environment (pH less than 4) and alkaline environment (pH more than 9). In acidic environment, aluminium metal dissolute at anode as ionic Al^{3+} form (Equation 2.11), while hydrogen will be reduced at cathode (Equation 2.12). In alkaline environment, aluminium metal dissolute at anode as ionic AlO_2^- form (Equation 2.13), while the oxygen is reduced at cathode (Equation 2.14). In the range between pH 4 to pH 9, aluminium is passivated by the formation of oxide layer on the exposed surfaces, hence provides the corrosion protection. In more negative potential (by forcing cathodic shift), aluminium reaches its immunity state where there will be no corrosion attack.

Oxidation at anode in acid: $\boldsymbol{Al \rightarrow\ Al^{3+} + 3e^{-}}$ **(2.11)**

Hydrogen reduction at cathode in acid: $\boldsymbol{2H^{+} +\ 2e^{-}\ \rightarrow\ H_2}$ **(2.12)**

Oxidation at anode in alkali**:** $\boldsymbol{Al_2O_2 + H_2O\ \rightarrow 2AlO_2^{-} + 2H^{+}}$ **(2.13)**

Oxygen reduction at cathode in alkali: $\boldsymbol{O_2 + 2H_2O +\ 4e^{-}\ \rightarrow 4OH^{-}}$ **(2.14)**

Different aluminium alloy has different corrosion tendency (J. R. Davis, 2001). Aluminium alloy 1xxx series has the highest corrosion resistance compared to the other aluminium alloy series because it has the lowest impurity in the alloy. The addition of new elements in the alloy reduces the corrosion resistance in the aluminium alloy. Aluminium alloy 2xxx series has the least corrosion resistant compared to the other aluminium series due to presence of copper in the alloy that create galvanic cell on its surface. Aluminium alloy 3xxx series has very high corrosion resistant since manganese does not create any significant site for corrosion process to take place. Aluminium alloy 4xxx series has good corrosion resistant because the silicon particle has very low corrosion current density. Aluminium alloy 5xxx series has very excellent corrosion resistance since magnesium dispersed uniformly to the matrix, protect the alloy from corrosion. However, alloys that contain 3% or more magnesium content are susceptible to stress corrosion cracking (Kishan Roodbari, 2015). Aluminium alloy 6xxx series has very good corrosion resistant magnesium and silicon does not affect the electrode potential in the alloy however, too high content of silicon that exceeds the formation of Mg_2Si may lead to intergranular corrosion.

Aluminium alloy 7xxx series is susceptible to stress corrosion cracking because the presence of zinc creates the galvanic cell on the alloy surface.

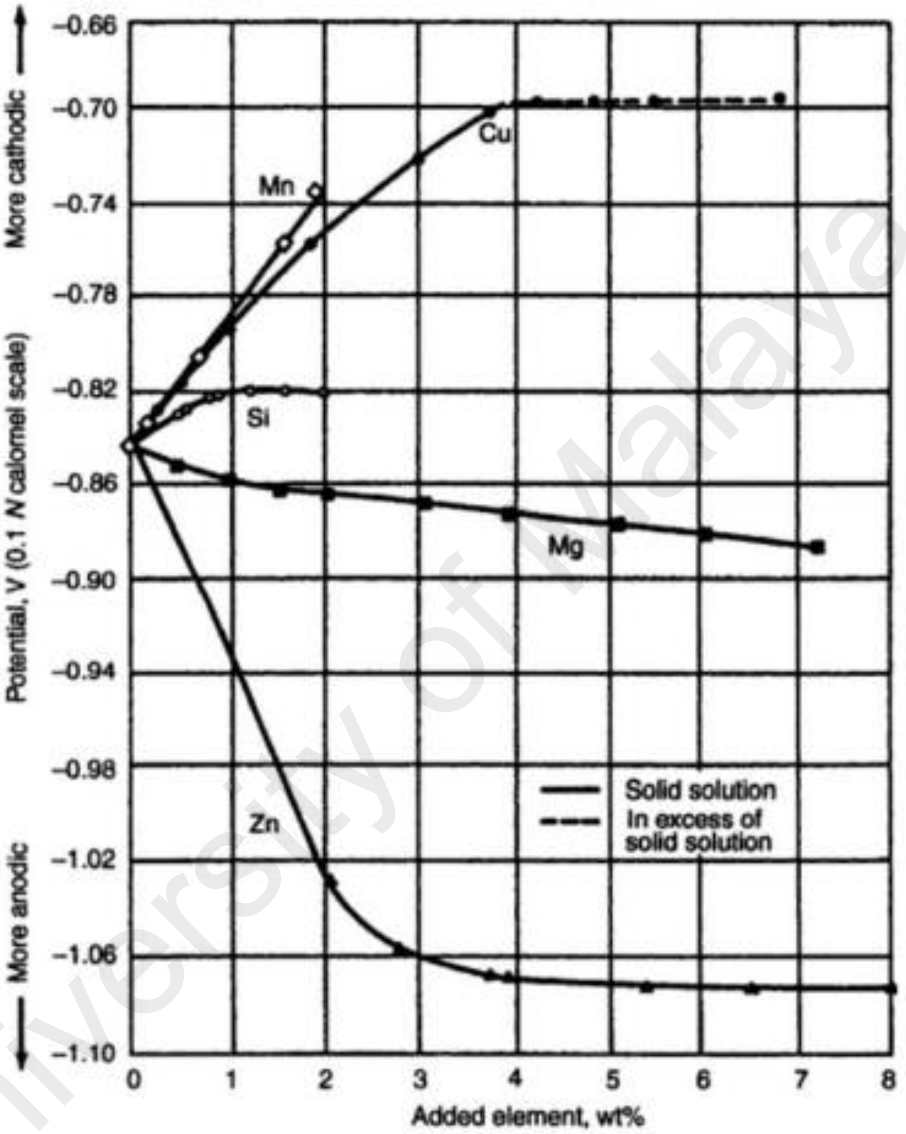

Figure 2.4 : Principle alloying element effect on the corrosion potential of aluminium alloy in electrolytic solution (J. R. Davis, 1999).

This study focus on the effect of alloying element towards the corrosion of aluminium alloys in Calophyllum inophyllum biodiesel. Different aluminium alloy is expected to have different corrosion behavior depending on the alloying element.

2.4.2.1 Pitting Corrosion in Aluminium Alloy

Pitting corrosion is a localized corrosion where the only certain area of the surface dissolute and a small hole is formed at the affected region. Aluminium produces oxide layer that protect the surface from having a direct contact with the environment. The behavior of pitting corrosion is hard to predict, so it is more dangerous that the uniform corrosion. Besides, it is hard to observe the pits at early stage because the size of pits appears to be small at the surface, but the corrosion may affect a huge region beneath the surface, deeper inside the metal surface. Sometimes, the small pit on the metal surface is covered with the corrosion product, so it is hard to detect the pitting corrosion until the metal starts to leak.

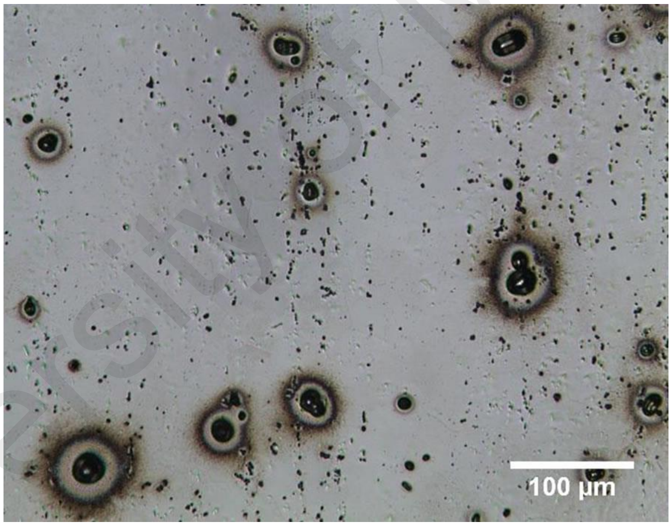

Figure 2.5 : Surface image of pitting corrosion on pure aluminium surface (Pereira, Silva, Acciari, Codaro, & Hein, 2012)

There are three reasons that can lead to pitting corrosion (Szklarska-Smialowska & ZS-Smialowska, 2005). First, pitting corrosion can occur due to the local chemical or mechanical damage on the protective layer of metal. Second, the metal that has non-uniform structure especially in alloy metal is more prone to pitting corrosion. Third, pitting corrosion can attack the surface region that has poor surface coating of metal. The pitting corrosion become more severe as the corrosion process is allowed to take place in a longer time. In general, there are three stages of pitting corrosion namely pitting initiation, pitting growth and pitting termination (leakage) (Figure 2.6). When mechanical effect involves in the reaction, there will be seven stages of pitting corrosion namely pit initiation stage, pitting growth stage, transition from pitting to fatigue crack nucleation stage, short crack growth stage, long crack growth stage and finally crack coalescence stage (F.-Y. Ma, 2012).

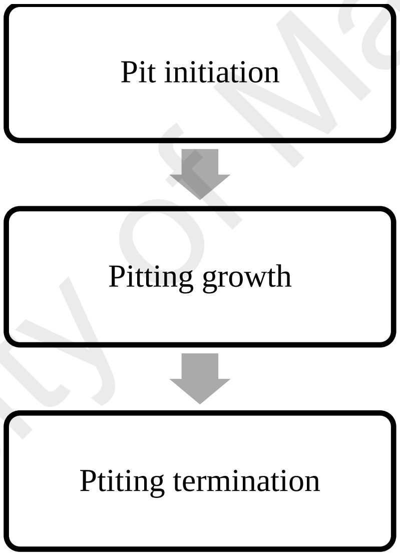

Figure 2.6 : Pitting corrosion process

Passive metal like aluminium produce an oxide layer to cover its surface from having a direct contact with the environment. Due to scratches that occur during the operation or aggressive chemical environment such as the presence of Cl^- ion, the oxide layer on that particular region damages, produce different aeration cell, thus allow the bare surface to have a direct contact to the environment. The first stage of pitting corrosion is known as pit initiation stage. In this stage, the aggressive anion such as Cl^- ion penetrates the protective oxide film, damages the protective film. So, the pit initiates on that surface and become anode before corroding the deeper site of metal sheet, while the surface that covered by protective film act as cathode. The second stage of pitting corrosion is known as pitting growth stage. The atoms below the initiated pit continue to dissolute, thus the pit become deeper beneath the metal surface and the wall become thinner. Then, the final stage of pitting corrosion is known as pitting termination. In this stage, the continuous dissolution of aluminium in pit bottom reaches its limit where the hole is form through the wall which leads to leaking.

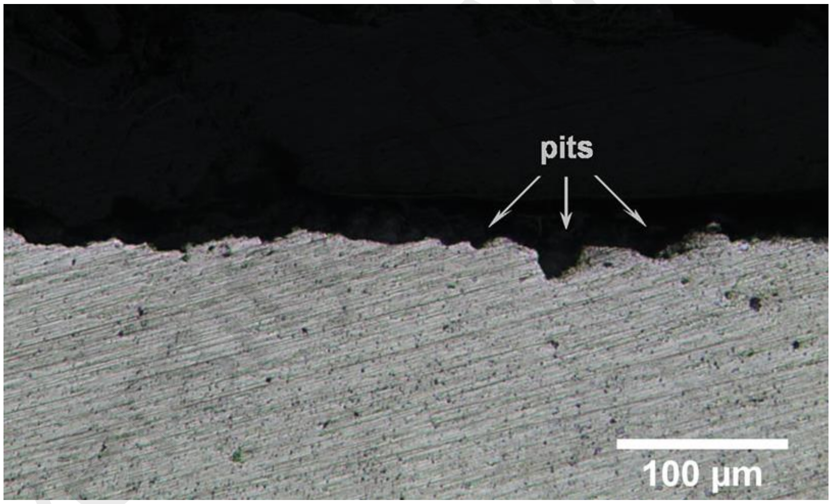

Figure 2.7 : Cross section image of pitting corrosion on pure aluminium surface (Pereira et al., 2012)

One of the factors that cause pitting in aluminium is the exposure to Cl^- ions (Pereira et al., 2012; Soltis, 2015; Szklarska-Smialowska, 1999). The study of pitting corrosion mechanism in aluminium alloy 1050 done by Pereira et al. by showed that the width of the pits are longer than the depth of the pits when immersed in NaCl (Pereira et al., 2012). This shows that the corrosion rate at wall of pits is higher that the corrosion rate at bottom of pits. Besides, Pereira et al. also concludes that the size and shape of pits depends on the immersion time in NaCl, the longer the immersion time will produce near conical and near hemispherical shaped pits while the shorter immersion time will produce hemispherical shaped pits.

When aluminium surface exposed to NaCl, Cl^- ion penetrates the oxide layer, react with aluminium surface by aluminium dissolution and initiate pits on the surface. Once the pit initiates on the surface, the pit grows depends on the rate of aluminium dissolution in pit cavity which is not affected by the Cl^- concentration in NaCl. Since more Cl^- ion penetrate the oxide layer, more pit initiation occur at the surface, hence the wider the pit form. Since more pit initiate on the surface, the corrosion rate of the exposed surface is higher compared to the pit bottom. As the exposure time increases, the corrosion rate increases slowly compared to the first hour. This explains the conical pitting shape form in aluminium.

2.5 Corrosion in Biodiesel

2.5.1 Biodiesel Production

Biodiesel is developed as an alternative to conventional petroleum diesel. Biodiesel has a lot of advantages such as non-toxic, low sulfur content, low greenhouse gases emission, renewable resources and improves lubricity (Haseeb, Sia, Fazal, & Masjuki, 2010). Biodiesel can be made from vegetable oils, animal fats or used cooking oil. In general, the feedstock of biodiesel can be classified into two which are edible oil and non-edible oil. Some sources of edible oil are coconut oil, peanut oil, sunflower oil, olive oil, soybean oil, rapeseed oil and palm oil (Antolın et al., 2002; Kaya et al., 2009; X. Liu, He, Wang, Zhu, & Piao, 2008; Nakpong & Wootthikanokkhan, 2010; Pleanjai & Gheewala, 2009; Rashid & Anwar, 2008; Sanchez & Vasudevan, 2006). Due to competition with food sources, non-edible oil has been developed from various sources such as croton megalocarpus, Pongamia pinnata, Madhuca indica, Calophyllum inophyllum, Jatropha curcas and rubber seed oil (Foidl, Foidl, Sanchez, Mittelbach, & Hackel, 1996; Ghadge & Raheman, 2005; Kafuku & Mbarawa, 2010; Naik, Meher, Naik, & Das, 2008; Ramadhas, Jayaraj, & Muraleedharan, 2005; Venkanna & Reddy, 2009). Beside corps, microalgae can also be utilized in biodiesel production (Chisti, 2007). Different countries focus on different feedstock sources of biodiesel depends on the geography of the country (Table 2.2).

The performance of biodiesel fuel is highly dependent on the fatty acid composition in the fuel. The primary contents of biodiesel are fatty acid and alcohol. In most cases, catalyst is also present to facilitate the biodiesel production. Transesterification technique is commonly used to produce biodiesel because the process is more economical and more efficient compared to the other techniques. During transesterification, triglycerides in vegetable oil are changed into monoglyceride. The end product of transesterification process is FAME and glycerol. FAME has the almost similar physical characteristics to petroleum diesel fuel, so it is suitable to be used in diesel engine.

Table 2.2 : Various potential feedstock for biodiesel around the world (Mahmudul et al., 2017)

Region	Country	Feedstock
North America	Ireland	frying oil, animal fats
	Canada	Rapeseed oil, Animal fat, Soybeans oil, Yellow grease and Tallow, Mustard oil
	Mexico	Animal fat, Waste Oil
	USA	Soybeans oil, waste oil, Peanut oil
	Cuba	Jatropha curcas, Moringa, Neem oil
South America	Argentina	Soybeans oil
	Brazil	Soybeans oil, Palm oil, Castor oil, Cotton oil
	Peru	Palm oil, Jatropha
Europe	Norway	Animal fats
	Sweden	Rapeseed oil
	France	Rapeseed oil, Sunflower oil
	Germany	Rapeseed oil
	Greece	Cottonseed oil
	Spain	Linseed oil, Sunflower oil
	Italy	Rapeseed oil, Sunflower oil
	Turkey	Sunflower oil, Rapeseed oil
	UK	Rapeseed oil, Waste cooking oil
Asia/ Southeast Asia	China	Jatropha, Waste cooking oil, Rapeseed oil
	Indonesia	Palm oil, Jatropha, Coconut oil
	India	Jatropha, Pongamia Pinnata, Soybean oil, Rapeseed oil, Sunflower oil
	Japan	Waste cooking oil
	Malaysia	Palm oil
	Philippines	Coconut oil, Jatropha
	Bangladesh	Rubber seed, Pongamia Pinnata
	Pakistan	Jatropha curcas
	Thailand	Palm oil, Jatropha, Coconut oil
	Iran	Palm oil, Jatropha, castor oil, Algae
	Singapore	Palm oil
Africa	Ghana	Palm oil
	Zimbabwe	Jatropha curcas
	Kenya	Castor oil
	Mali	Jatropha curcas
Australia and Oceania	Australia	Beauty leaf, Jatropha curcas, Pongamia, waste cooking oil, animal tallow

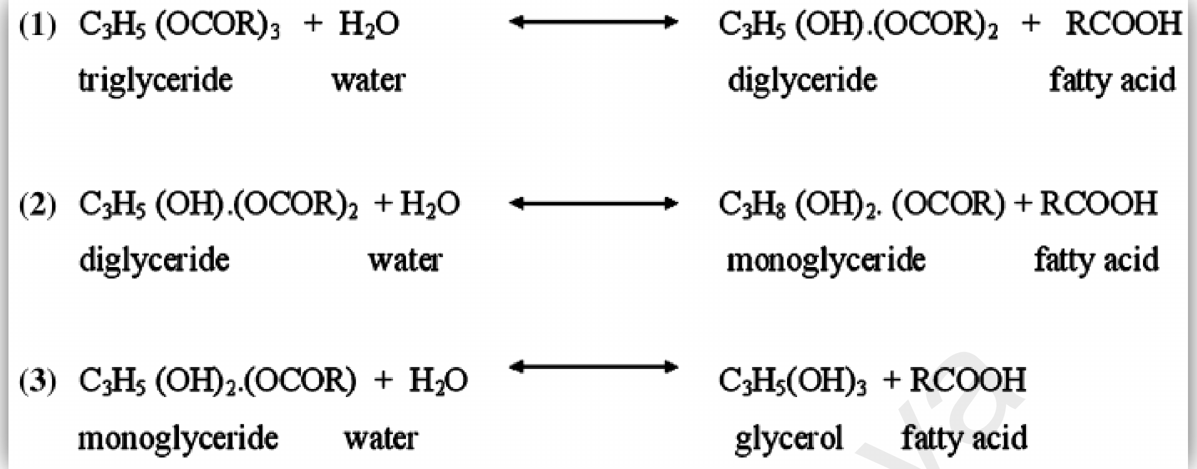

(1) $C_3H_5(OCOR)_3 + H_2O \longleftrightarrow C_3H_5(OH).(OCOR)_2 + RCOOH$

triglyceride water diglyceride fatty acid

(2) $C_3H_5(OH).(OCOR)_2 + H_2O \longleftrightarrow C_3H_8(OH)_2.(OCOR) + RCOOH$

diglyceride water monoglyceride fatty acid

(3) $C_3H_5(OH)_2.(OCOR) + H_2O \longleftrightarrow C_3H_5(OH)_3 + RCOOH$

monoglyceride water glycerol fatty acid

Figure 2.8 : Chemical reaction during transesterification process (Alenezi, Baig, Wang, Santos, & Leeke, 2010)

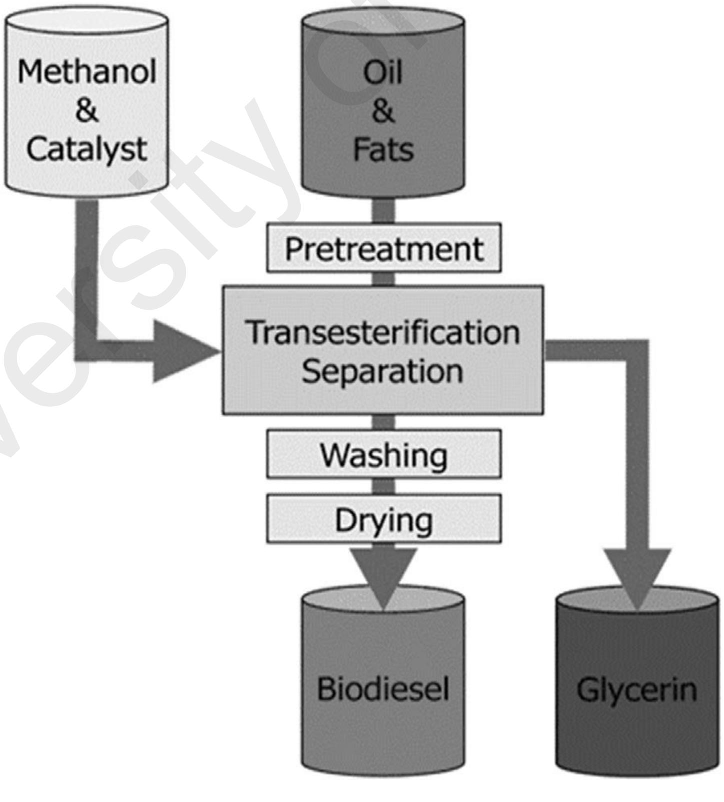

Figure 2.9 : Flow chat of transesterification process in biodiesel production (Mofijur et al., 2016)

The application of raw biodiesel can cause some problems to the engine such as corrosion and fuel filter clog. In order to reduce the problems in engine, biodiesel blends where the raw vegetable oil are mixed with petroleum diesel usually the percentage of biodiesel dented by capital B is recommended by researchers. The production of biodiesel must obey the industry standard ASTM D6751 for B100, 100 percent biodiesel and ASTM D7467 for B6, 6 percent biodiesel to B20, 20 percent biodiesel that concerns on the glycerin content in biodiesel and biodiesel stability during storage (Table 2.3). Some important characteristics in biodiesel are cetane number, sulphate ash, acid number, free glycerin, oxidation stability, water and sediment content, methanol content, flash point and sulfur content.

Table 2.3 : Comparison the properties of fuel of biodiesel B100, B6 to B20 and Diesel based on ASTM D6751, ASTM D7467 and ASTM D975 respectively (Testing & Materials, 2010).

Property	Biodiesel B100 (ASTM D6751)	Biodiesel B6 to B20 (ASTM D7467)	Diesel (ASTM D975)
Acid Number, mg KOH/g	0.3 max	0.3	-
Flash point, ^{0}C	130 min	52 min	52 min
Water and Sediment, % vol.	0.05 max	0.05 max	0.05 max
Ash content, mass %	0.02 max	0.01 max	0.01 max
Cetane number	47 min	40 min	40 min
Sulfur, mass %	0.015	0.05	0.05
Oxidation stability, hours	3 min	6 min	-
Copper strip corrosion	No. 3	No. 3	No. 3
Carbon residue, mass %	0.05 max	0.35 max	0.15
Free glycerin, mass %	0.02	-	-
Total glycerin, mass %	0.24	-	-

Cetane number measures the combustion behavior of fuel under certain pressure and temperature. High cetane number shows that the fuel has smoother combustion. In biodiesel, cetane number is highly dependent to fatty acid carbon chain; the longer the fatty acid carbon chain, the higher the cetane number (Van Gerpen, 1996). Sulphate ash measures the content of metal and other inorganic contaminants in fuel that can be found in three forms which are abrasive solids, soluble metallic soaps and residual biodiesel catalysts. High content of these compounds can cause filter clog after the fuel combustion. Acid number measures the free fatty acid content in biofuel usually expressed as the required mass of potassium hydroxide, KOH to neutralize FAME. The SI unit of acid number is mg KOH/g. There are three types of fatty acid methyl, FAME ester in biodiesel which are known as oleic acid, linoleic acid and linolenic acid (Figure 2.10). High acid number indicates that the fuel contain a lot of free fatty acid that can cause severe corrosion in engine. Free glycerin in biodiesel may be separated from biodiesel and sink at the bottom of the tank and attracts the water, monoglycerides and soaps which can cause damage to vehicle fuel injection system. Flash point measures of the lowest temperature of the fuel can ignite when exposed to flame which relates to the safety. High flash point number indicates that the fuel is hard to ignite, so the safer the fuel. In biodiesel, flash point increases as the content of vegetable oil in biodiesel blends increases (Mattos, Bastos, & Tubino, 2015). Oxidation stability determines the susceptibility of the fuel to oxidize. The oxidation in biodiesel is higher when the content of unsaturated fatty acid chain is higher in the fuel (Yaakob, Narayanan, & Padikkaparambil, 2014). Water content and sediment content in biodiesel allows the biological growth, forms sludge and slums that can convert biodiesel into free fatty acid through hydrolysis reaction that can causes corrosion (Ziółkowska & Wardzińska, 2015).

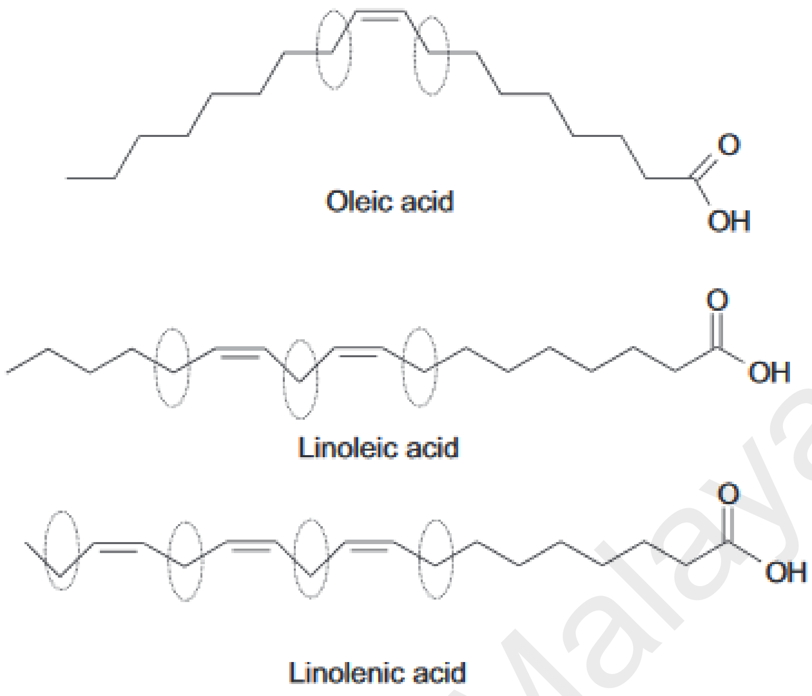

Figure 2.10 : Three common FAME molecular structures in biodiesel.

2.5.2 Calophyllum Inophyllum Biodiesel

Calophyllum inophyllum is one of the non-edible biodiesel feedstock that has been developed in order to avoid the competition between biodiesel feedstock source and food source (Agoramoorthy, Sarnaik, Mungikar, Punde, & Hsu, 2012; Atabani & da Silva César, 2014; Fattah et al., 2014; Jahirul et al., 2014). Calophyllum inophyllum oil can be extracted from seeds of calophyllum inophyllum that mostly populated in East Africa, India, South East Asia, Australia and South Pacific, grows best on sand that usually located near to the seashore, and also can grow on clay, calcareous soils and rocky soils (Atabani & da Silva César, 2014).

Figure 2.11 : Calophyllum inophyllum tree grows on sand (Friday & Okano, 2006)

Calophyllum inophyllum is commonly known as Bintangor or Penaga Laut in Malaysia, has low branches, shiny leaves, fragrant white flowers and fruits (Figure 2.12-2.13). Some parts of Calophyllum inophyllum such as bark, leaves and seeds are useful for medicinal purposes but the matured fruit is poisonous that can cause nausea, diarrhea and dehydration (Koh, 2009; Nelson, Shih, Balick, & Lampe, 2007).

Figure 2.12 : Calophyllum inophyllum fragrant white flowers that flowering heaviest in the late spring and early summer (Friday & Okano, 2006)

Figure 2.13 : Nearly matured fruit of Calophyllum inophyllum (Friday & Okano, 2006)

Malaysia is one of the native habitats of Calophyllum inophyllum in the world. Warm climate, abundant rainfall throughout the year and a lot of sandy soil along the beaches in Malaysia provides the optimum condition for the Calophyllum inophyllum to grow in Malaysia. Malaysia has a great potential to develop calophyllum inophyllum biodiesel since the feedstock can be obtained easily. The development of Calophyllum inophyllum in Malaysia can also reduce the dependency on palm biodiesel, so, the competition for food can be reduced as palm is also one of the main food sources in Malaysia.

Before producing biodiesel, the crude oil must be extracted from Calophyllum inophyllum seed first. First, the seeds were dried in the presence of sunlight for two to three days. Then, the kernel is separated from the shell, stored at controlled temperature of 26 ^{o}C to 27 ^{o}C with controlled humidity at 60% to 70% humidity in order to optimize the the oil yield. Next, the kernel is pressed by using pressing machine to extract the oil.

Figure 2.14 : Dried seeds of Calophyllum inophyllum (Atabani & da Silva César, 2014)

Figure 2.15 : Separation of dried kernel from shell of dried Clophyllum inophyllum seeds (Atabani & da Silva César, 2014)

Later, the Calophyllum inophyllum oil undergoes four processes in order to produce Calophyllum inophyllum biodiesel (Ashok, Nanthagopal, & Vignesh, 2017; Atabani & da Silva César, 2014) (Figure 2.16). The first process is known as pre-treatment process. In pre-treatment process, the Calophyllum inophyllum oil is heated in rotary evaporator to remove the moisture in the oil. Then, the Calophyllum inophyllum oil undergoes esterification process. During esterification process, Calophyllum inophyllum is converted into Calophyllum inophyllum methyl ester. Next, the third stage of Calophyllum inophyllum biodiesel production is transesterification. In transesterification, esterified

Calophyllum inophyllum reacts with methanol and alkaline potassium hydroxide, KOH as the catalyst. The end product of this reaction is methyl ester and glygerol. At the end of this process, glycerol and impurities are removed from the biodiesel. Finally, Calophyllum biodiesel undergoes post treatment process where the impurities, methanol and water in the biodiesel are removed by using distilled water. The property and fatty acid composition of Calophyllum inophyllum biodiesel is shown in Table 2.4 and Table 2.5 respectively.

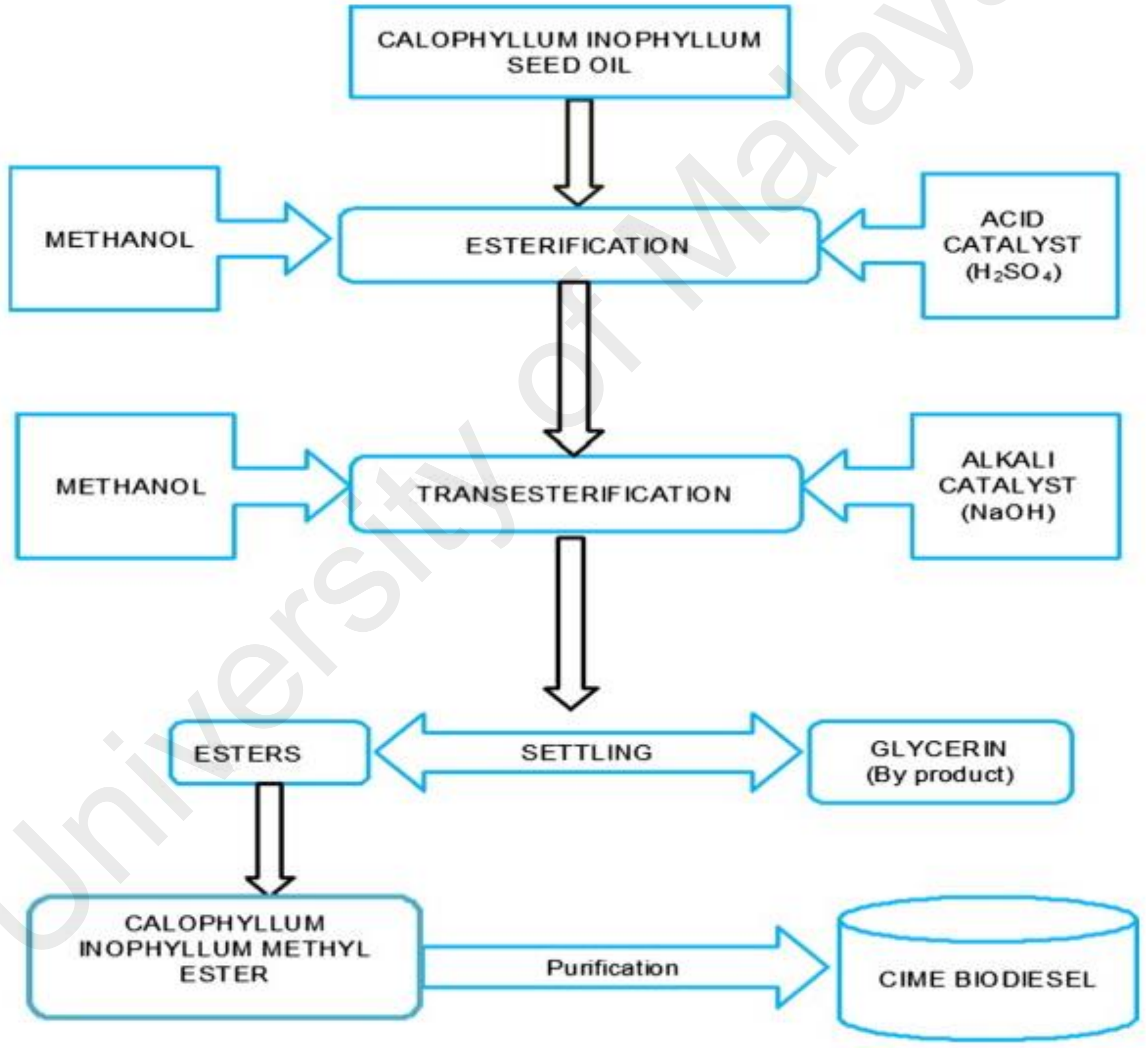

Figure 2.16 : Process involves in Calphyllum inophyllum biodiesel production (Ashok et al., 2017)

Table 2.4 : Properties of Calophyllum inphyllum biodiesel developed by Atabani et al. (Atabani et al., 2013)

Property	Unit	Value
Density at 40 °C	kg/m^3	877.6
Kinematic viscosity at 40 °C	mm^2/s	5.5377
Oxidation stability	hour at 110 °C	6.12
Cloud point	°C	12
Flash point	°C	162.5
Copper strip corrosion	-	1a
Calorific value	kJ/kg	39,513
Sulfur	Ppm	4.11

Table 2.5: Fatty acid composition of Calophyllum inophyllum biodiesel (Jahirul et al., 2014)

Fatty Acid	Carbon Formula	Weight Percentage, %
Palmitic	C16:0	13.66
Palmitoleic	C16:1	0.24
Heptadecanoic	C17:0	0.15
Heptadecanoic	C17:1	0.06
Stearic	C18:0	16.55
Oleic	C18:1	42.48
Linoleic	C18.2	25.56
Linolenic	C18:3	0.20
Arachidic	C20:0	0.87
Arachidonic	C20:1	0.23

2.5.3 Corrosion Mechanism in Biodiesel

Corrosion in biodiesel can occur when the metal surface is in contact to the biodiesel fuel. The susceptibility of corrosion in biodiesel is closely related to the oxidation stability of biodiesel. The presence of contaminants in biodiesel such as glycerol, free fatty acid and metals due to incomplete process may lead to oxidation instability (Banga & Varshney, 2010). There are three stages involves in the oxidation process of biodiesel which are initiation, propagation and termination (Pullen & Saeed, 2012; Zuleta, Baena, Rios, & Calderón, 2012) (Figure 2.17).

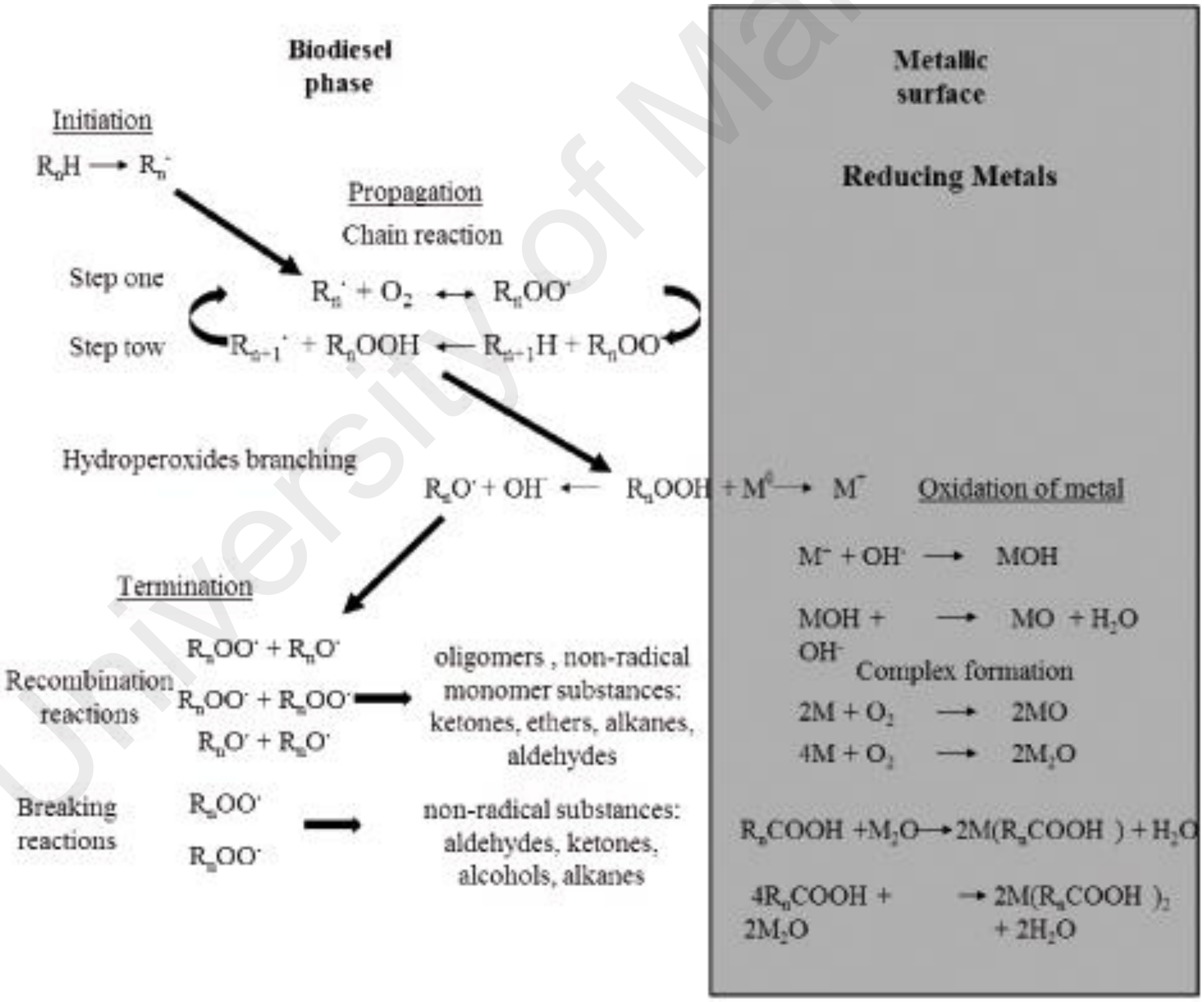

Figure 2.17 : Three stages involved in the oxidation of biodiesel (Zuleta et al., 2012)

The first stage of the biodiesel oxidation is initiation stage. In initiation stage, unsaturated fatty acid chains forms a new carbon based fatty acid radical, R* from the reaction between initiator radical, I* and unsaturated fatty acid chain (Pullen & Saeed, 2012). This reaction removes the hydrogen atoms from unsaturated fatty acid chain. The presence of initiator radical, I* is most probably from the catalyst used in transesterification process(Pullen & Saeed, 2012). The second stage of biodiesel oxidation is propagation stage. In propagation stage, there are two steps involved in this stage. First, the fatty acid radical, R* forms the unstable fatty acid peroxide radical, ROO* from the reaction with oxygen molecules. Then, the unstable fatty acid peroxide radical, ROO* form fatty acid hydro peroxide or allylic hydroperoxide, ROOH* and new allyl radical, R_{n+1}* from the reaction with the original unsaturated fatty acid chain. The final stage of biodiesel oxidation is termination stage. In termination stage, stable polymer chains are produced from the the reaction of the two radicals. The end product of this stage is non-radical substances such as alcohols, ketones, esters, organic acids and etc. The oxidation of biodiesel causes some biodiesel properties changes that can affect the quality of biodiesel such as acid number, peroxide value, viscosity, iodine value and FAME content. The increase on acid number due to oxidation process can increase the corrosive property of biodiesel.

Water and fatty acid content in biodiesel are the main causes of corrosion in biodiesel. During transesterification process, there are a lot of contaminants present in biodiesel. Final washing of biodiesel must be done to remove the impurities in biodiesel. Water washing step is involved in the biodiesel purification to remove sodium salts and soaps and later it will be reduced in drying process (A. Sarin, 2012). However, due to hygroscopic properties of FAME, some water molecules are attracted to the FAME chains in biodiesel by hydrolysis process. Over a period of time, water accumulates and form a thin layer sink at the bottom of the fuel storage tank. Water act as an electrolyte while metal act as anode and cathode. The corrosion between metal and water is shown in Equation 2.15 – 2.17.

Reaction at anode: $\boldsymbol{M \rightarrow M^{n+} + ne^-}$ **(2.15)**

Reaction at cathode: $\boldsymbol{O_2 + 2H_2O + 4e^- \rightarrow 4OH^-}$ **(2.16)**

$$\boldsymbol{2H_2O + 2e^- \rightarrow H_2 + 2OH^-} \quad \textbf{(2.17)}$$

Studies show that biodiesel is more corrosive compared to petroleum diesel. Fazal et al. found out that the corrosion rate of copper is higher than aluminium when immersed in pure palm biodiesel compared to pure petroleum biodiesel at 80 ^{o}C while there was no significant different in corrosion rate for stainless steel (Fazal et al., 2010). Acid produced from palm biodiesel at high temperature react with copper and produce different acids like 9-octadecenoic acid, octanoic acid, nonanoic acid, hexadecanoic acid, 9-octadecanoic acid that are more corrosive compared to the palm biodiesel alone without copper, hence the corrosion rate of copper is highest compared to the other metals.

Jin et al. obtained the same result as Fazal et al. when the ASTM 1045 mild steel is immersed in pure palm biodiesel, the rate of corrosion is higher compared to pure petroleum diesel as the temperature and immersion period increases might be due to the presence of the high concentration of oxidizable components of palm biodiesel like unsaturated fatty acid and active atom oxygen with the rising temperature and longer time exposure (Jin et al., 2015). Haseeb et al. observed that the corrosion rates of copper is higher compared to leaded bronze as the concentration of palm biodiesel blend increases at room temperature and 60 ^{o}C (Haseeb, Masjuki, et al., 2010). Leaded bronze seems to have a better corrosion resistance compared to copper due to the presence of the alloying elements. Another study done by Thangavelu et al. by immersing mild steel, copper and aluminium into various palm biodiesel-diesel-ethanol fuel blends at room temperature and 60 ^{o}C showed that copper that exposed to the highest ethanol content in fuel blend has the highest corrosion rate due to high concentration of water and oxygen in ethanol that speed up the rate of corrosion of copper at higher ethanol composition in fuel blends (Thangavelu et al., 2016).

Beside palm biodiesel, rapeseed biodiesel also show the same pattern. Su et al. observed that the corrosion rate of aluminium, copper and iron increases with the increase of rapeseed biodiesel blends at room temperature for 90 days where iron has the highest corrosion rate compared to aluminium and copper (Su et al., 2014). It is believed that the rapeseed biodiesel molecular structure contains a lot of double bonds that can oxidize easily and react with metals to produce aldehydes, ketones and other corrosive substance. Another study done by Hu et al. also proved that the rapeseed biodiesel are more corrosive than petroleum diesel during the immersion of copper, carbon steel, aluminium and stainless steel in rapeseed biodiesel at 43 ^{o}C (Hu et al., 2012). Among the four metals, the corrosion rate of copper and carbon steel are worse compared to aluminium and stainless steel because copper and carbon steel more prone to oxidized when exposed to biodiesel while aluminium and stainless steel tend to form metal oxide films that can prevent metals from oxidation.

A corrosion study of metal parts of diesel engine namely piston metal and piston liner metal in various non-edible biodiesel from seeds oils originated in India namely Jatropha curcas, Pongamia glabra, Madhuca indica and Salvadora oleoides that has been carried out by Kaul et al. for 300 days at the monitored temperature between 15 ^{o}C to 40 ^{o}C showed that the corrosion rate of metals in four biodiesel are higher compared to the petroleum diesel where the metal immersed in Salvadora oleoides has the highest corrosion rate followed by Jatropha curcas due to high sulfur content in Salvadora oleoides and high concentration of fatty acid in Salvadora oleoides that enhance the oxidization of metal compared to the other biodiesel (Kaul et al., 2007).

Until today, there is no study on the corrosion property of Calophyllum inophyllum biodiesel have been done. According to the other studies mention above, the main factor that leads to the corrosivity of biodiesel is highly dependent to the fatty acid content in the biodiesel. Since Calophyllum inophyllum biodiesel contain almost the same fatty acid content as in other biodiesels, it is expected to be more corrosive compared to the petroleum diesel at the end of this study. In this study, the effect of the concentration of fatty acid towards the corrosive behavior of Calophyllum inophyllum will be studied. So, the various Calophyllum inophyllum biodiesel blends will be prepared to study the corrosion effect.

2.6 Corrosion Characterization Technique

2.6.1 Weight Loss Analysis

In 1866, Calvert and Johnson figured out the method to remove the zinc from brass by immersing the brass in the sulphuric acid for several days (Baboian, 1995). According to Calvert and Johnson, during the immersion of brass in sulphuric acid, one element from brass which is zinc is dissolved in the acid, while the other elements in brass are remained. The concept of dealloying is later deployed in studying the corrosion rate.

When a metal is exposed to the electrolyte or corrosive environment, the local action cells react to the electrolyte where anode region undergo oxidation process and cathode region undergo reduction process. During oxidation process, metal atom at anode loss its valence electron, thus become cation. The electron flows within the local action cells through the metal itself, while the cation dissolve in the electrolyte and form a new bond with anion that move freely in the electrolyte and produce a new compound. The oxidation of atoms at anode reduces the number of atom in metal, thus the atomic mass of metal reduces and the weight of metal decreases.

In weight loss analysis technique, the study of corrosion rate is calculated by measuring the amount of weight loss of metal during the metal immersion in the electrolyte or solution for a certain period of time. The relationship between the mass loss and the corrosion rate is clearly shown by Faraday's Law (Equation 2.18).

$$\boldsymbol{r = \frac{K \times w}{A \times t \times \rho}} \qquad \textbf{(2.18)}$$

Where r is the corrosion rate, K is corrosion constant (Table 2.6), w is metal weight loss in grams, A is the surface area exposed to the electrolyte in cm^2, t is time exposed to the electrolyte or solution in hours and ρ is the density of metal in g/cm^3. The corrosion rate unit is depends on the constant K (Table 2.6).

Table 2.6: Corrosion rate unit based on constant K value. (Metals, 2011)

Corrosion Rate Unit	Constant (K) Value
mils per year (mpy)	3.45×10^6
inches per year (ipy)	3.45×10^3
inches per month (ipm)	2.87×10^2
millimeters per year (mm/y)	8.76×10^4
micrometers per year (um/y)	8.76×10^7
picometers per second (pm/s)	2.78×10^6
grams per square meter per hour (g/m2·h)	$1.00 \times 10^4 \times \rho$
milligrams per square decimeter per day (mdd)	$2.10 \times 10^6 \times \rho$
micrograms per square meter per second (μg/m2·s)	$2.78 \times 10^6 \times \rho$

The advantages of weight loss analysis technique are the procedure is simple and cheap, does not require sophisticated equipment, demonstrate the real situation and allow the analysis of the corrosion product. However, disadvantages of weight loss analysis technique are it requires a long period of immersion time to get accurate result and hard to detect the small corrosion rate for instance pitting, that occur without significant change in mass.

CHAPTER 3: METHODOLOGY

3.1 Overview

In this chapter, the procedure of the experiment for corrosion study will be explained. In this study, static immersion technique will be used to identify the corrosion rate between the aluminium alloys and Calophyllum inophylum biodiesel blends. The procedure of the static immersion test technique is shown in Figure 3.1.

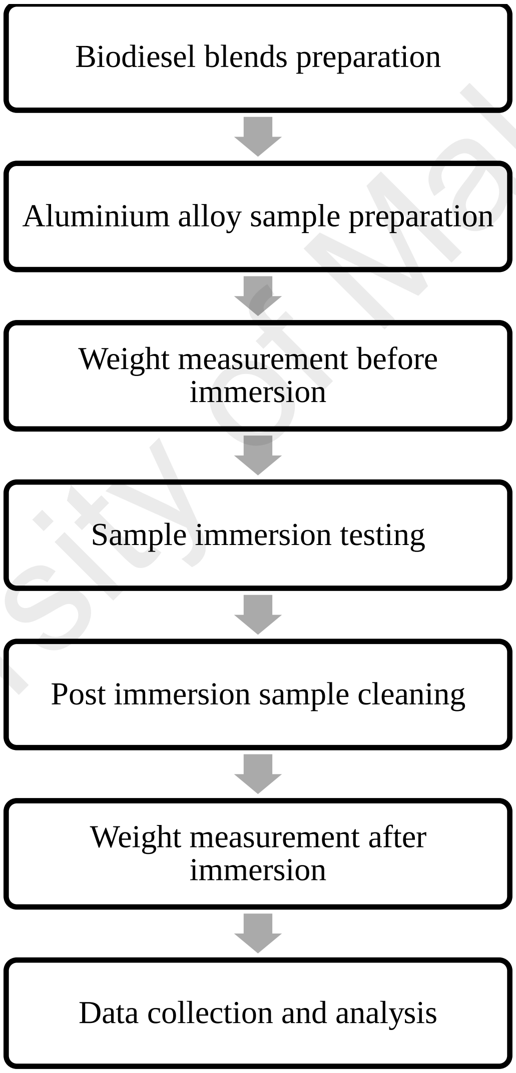

Figure 3.1 : Procedure of static immersion test technique for corrosion study.

Next, the corrosion image of the samples is characterized by using SEM. The image of the surface of the samples before and after the immersion test in various Calophyllum inophyllum blends are compared to study the severity of corrosion occur on the surface of the samples. From the comparison of the image of samples before and after immersion test, the morphology of the corrosion of aluminium alloy samples in various Calophyllum inophyllum biodiesel blends can be studied.

3.2 Biodiesel Blends Preparation

In this study, three Calophyllum inophyllum biodiesel blends are prepared which are B5, B10 and B15. First, the required amount of each Calophyllum inophyllum biodiesel and commercial diesel is calculated and measured using measuring cylinder. The concentration of Calophyllum inophyllum biodiesel in the biodiesel blends is highly determined by 'B' number. For instance, Calophyllum inophyllum biodiesel B5 blend is made up of 5 percent of Calophyllum inophyllum biodiesel and 95 percent of commercial diesel, while the content of Calophyllum inophyllum biodiesel B10 blend is made up of 10 percent of Calophyllum inophyllum biodiesel and 90 percent of commercial diesel. For Calophyllum inophyllum biodiesel B15 blend, 15 percent of Calophyllum inophyllum biodiesel and 85 percent of commercial diesel is required. The fuel properties of Calophyllum inophyllum biodiesel B100 is shown in Table 3.1.

Table 3.1 : Fuel properties of Calophyllum inophyllum biodiesel (Ong, Mahlia, Masjuki, & Norhasyima, 2011)

Properties	Unit	Value
Density at 15 ^{o}C	kg/m^3	869
Cetane number	-	57
Viscosity at 40 ◦C	mm^2/s	4.0
Flash point	^{o}C	140
Cloud point	^{o}C	13.2
Calorific value	kJ/kg	41,397
Water content	wt%	0.005
Acid value	mgKOH/g	1.62

Figure 3.2 : Calophyllum inophyllum biodiesel B100 obtained from University of Malaya.

Then, Calophyllum inophyllum biodiesel and commercial biodiesel is mixed according to the calculated volume required for each blends. After mixing, the Calophyllum inophyllum biodiesel blends are stirred by using Fisher Scientific Isotemp Heated Magnetic Stirrer / Hotplate (Figure 3.3). Calophyllum inophyllum biodiesel blends are allowed to be stirred for 30 minutes at room temperature. Each Calophyllum inophyllum biodiesel blends are labeled and stored in the laboratory glass bottle (Figure 3.4). The kinetic viscosity, dynamic viscosity and density of Calophyllum inophyllum biodiesel blends is shown in Table 3.2.

Table 3.2: Kinetic viscosity, dynamic viscosity and density of Calophyllum inophyllum biodiesel blends.

Biodiesel blends	B0	B5	B10	B15
Kinetic viscosity at 40 ^{o}C (mm^{2}/s)	3.3943	3.4368	3.4649	3.5929
Dynamic viscosity at 40 ^{o}C (mPa.s)	2.8196	2.8629	2.8927	4.2656
Density at 40 ^{o}C (g/cm^{3})	0.8307	0.8330	0.8349	0.8683

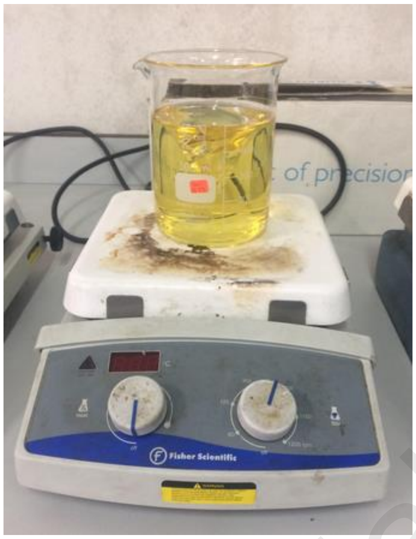

Figure 3.3 : Calophyllum inophyllum biodiesel blend is stirred using magnetic stirrer Fisher Scientific Isotemp Heated Magnetic Stirrer / Hotplate

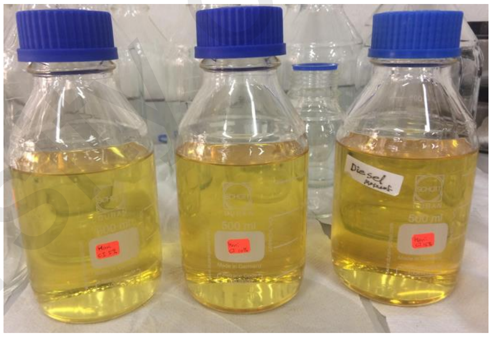

Figure 3.4 : Three Calophyllum inophyllum biodiesel blends, B5 (left), B10 (middle) and B15 (right)

3.3 Sample Preparation

In this study, three aluminium alloys have been used as sample for corrosion study in different Calophyllum inophyllum biodiesel blends which are aluminium alloy 3003, 5052 and 6061 (Table 3.3).

Table 3.3 : Chemical composition of aluminium alloy 3003, 5052 and 6061 (A. Association, 2009)

Aluminium alloy	3003	5052	6061
Si, %	0.6	0.25	0.8
Fe, %	0.7	0.40	0.7
Cu, %	0.20	0.10	0.40
Mn, %	1.5	0.10	0.15
Mg, %	-	2.8	1.2
Cr, %	-	0.35	0.35
Ni, %	-	-	-
Zn, %	0.10	0.10	0.25
Ti, %	-	-	0.15
Others, %	0.15	0.15	0.15
Al, %	96.75	95.75	95.85

First, aluminium alloys with the thickness of 4mm are cut into a square shaped with length of 1 inch by width of 1 inch (Figure 3.5). Then, the samples are grinded using grit paper grade 600 and 800 to remove the oxide layer on the surface of the samples. The samples are rinsed with distilled water after grinding. Finally, the samples are degreased with ethanol to remove the contaminants on the surface of the sample and dried at the room temperature.

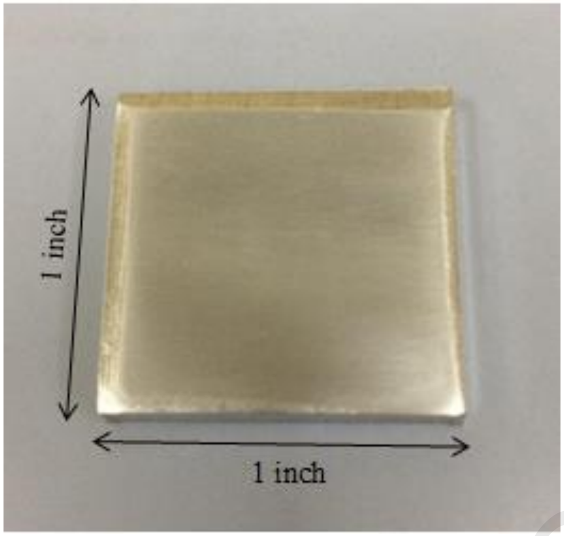

Figure 3.5 : Aluminium alloy sample (1 inch x 1 inch) for static immersion test.

During the grinding process, the rough scratches are eliminated from the surface, hence the surface will be appeared smoothly with even surface roughness. The even surface roughness is important in corrosion testing. The presence of deep scratches and uneven roughness will affect the result of corrosion study since the scratch region tends to be anode, thus the corrosion will be initiated at the scratch region. So, the result of corrosion study will be affected by scratches and uneven surface factor and may not be reliable.

3.4 Immersion Test

In this study, the static immersion test technique is used to obtain the corrosion rate between aluminium alloys and Calophyllum inophyllum biodiesel blends. The weight loss is determined by weight difference before and after immersion. The amount of weight loss is closely related to the corrosion rate.

Before starting the static immersion test, the samples are weighed by using Sartorius Digital Weighing Scale (Figure 3.6). The weight is measured in gram up to 4 decimal places accuracy. The weight readings of each sample before immersion test are recorded and will be compared to the weigh readings of samples after immersion test.

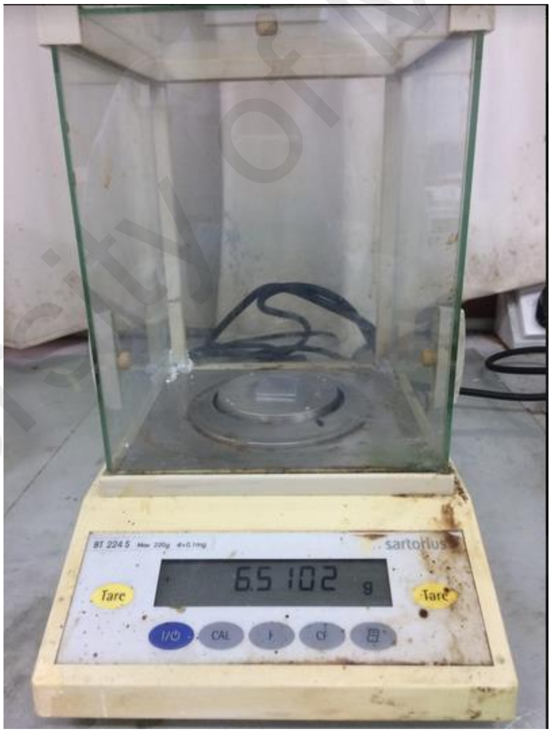

Figure 3.6 : Aluminium alloy sample is weighed using Sartorius Digital Weighing Scale.

After weighing the samples, the sample is immersed into the Calophyllum inophyllum biodiesel blends which are B0, B5, B10 and B15 for 1200 hours at room temperature (Figure 3.7). The immersion test is repeated for three times to obtain more accurate and consistent result.

Figure 3.7 : Aluminium alloy samples immersed in various Calophyllum inophyllum biodiesel blends

3.4.1 Post Immersion Sample Cleaning

After immersion test, the weight of the samples is measured again and compared with the weight before immersion test to identify the weight loss due to the reaction between aluminium alloy sample and Calophyllum inophyllum biodiesel blends. In order to obtain accurate weight measurement, the samples need to be cleaned first before measuring weight to remove any corrosion product on the surface of the samples.

There are three categories of cleaning the samples after immersion test which are chemical, mechanical and electrolytic. After removing of the aluminium alloy sample from Calophyllum inophyllum biodiesel blends, the corrosion prodcuts are removed by using chemical method first by immersing the samples in dilute nitric acid (about 10% concentration) for a few seconds. Then, the corrosion products are removed by using mechanical method by brushing the surface of samples using non-metallic bristle to remove the excess corrosion product. The sample is rinsed with distilled water after the brushing process. Finally, the corrosion products are removed by using electrolytic method by using ultrasonic cleaner (Figure 3.8).

Figure 3.8 : Ultrasonic cleaner used to clean the sample after immersion test.

3.4.2 Data Collection and Analysis

In static immersion test, the weight of each aluminium alloy sample before immersion and after immersion is taken. From the data, the weight loss, W_{loss} of the aluminiujm alloy sample from the immersion test is identified (Equation 3.1).

$$W_{loss} = W_i - W_f \quad \textbf{(3.1)}$$

Where W_{loss} is weight loss, W_i is weight before immersion and W_f is weight after immersion. The experiment is repeated for three times to get more accurate and consistent result. So, the average weight loss, $W_{loss,avg}$ from the three repeating samples of the same parameter is determined (Equation 3.2).

$$W_{loss,avg} = \frac{W_{loss,1} + W_{loss,2} + W_{loss,3}}{3} \quad \textbf{(3.2)}$$

Where $W_{loss,avg}$ is average weight loss, $W_{loss,1}$ is weight loss of sample of the first experiment, $W_{loss,2}$ is the weight loss of the sample of the second repetition of the experiment and $W_{loss,3}$ is the weight loss of the sample of the third repetition of the experiment. Then, the corrosion rate of the samples, r is identified by dividing the average weight loss of the sample, $W_{loss,avg}$ with immersion period, t and surface area exposed to Calophyllum inophyllum biodiesel blends (Equation 3.3).

$$r = \frac{W_{loss,avg}}{t \times A} \quad \textbf{(3.3)}$$

3.5 Surface Characterization

3.5.1 Scanning Electron Microscope (SEM)

The image of surface of aluminium alloy samples can be observed and captured by using PHENOM ProX table top SEM at high magnification. The image of the surface of the samples is projected by SEM from the interaction between the primary electron beam and samples. The magnification, brightness and contrast is controlled to obtain the good quality of surface image when using SEM.

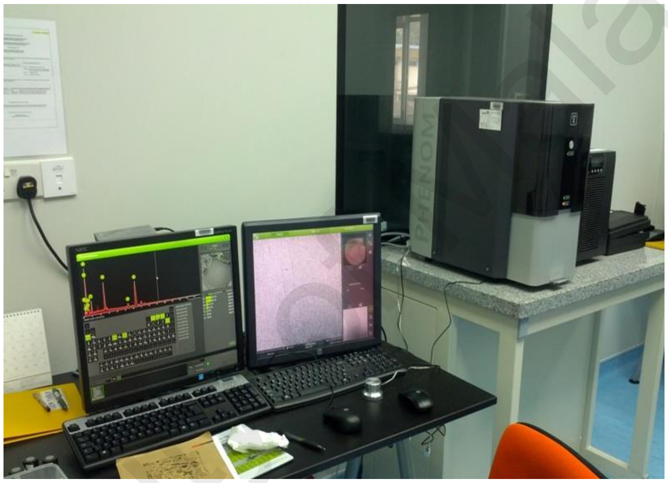

Figure 3.9 : PHENOM ProX table top SEM available in University of Malaya

In this study, the image of the surface of samples after immersion test is observed and captured using scanning electron microscopy, SEM. Then, the image of polished raw samples (without immersion test) is also observed and captured by using scanning electron microscopy, SEM at the same magnification setup as a reference. Finally, the image of immersed sample is compared to the raw sample to study the corrosion morphology.

CHAPTER 4: RESULTS AND DISCUSSION

4.1 Overview

In this chapter, the result from immersion test and SEM will be explained. In immersion test, the corrosion rate of aluminium alloy 3003, 5052 and 6061 immersed in Calophyllum inophyllum biodiesel blends B0, B5, B10 and B15 is obtained from weight loss after the immersion test for 1200 hours at room temperature. The corrosion behavior of aluminium alloy 3003, 5052 and 6061 in Calophyllum inophyllum biodiesel blends will be described from the observation of surface image after the immersion test. The surface image is observed and captured by using SEM.

4.2 Immersion Test

In immersion test, the weight loss is taken three times for each parameter in order to obtain more consistent and accurate result and recorded (Appendix A). The weight loss of aluminium alloys 3003, 5052 and 6061 after the immersion test in Calophyllum inophyllum biodiesel blends B0, B5, B10 and B15 at room temperature for 1200 h are calculated by using Equation 3.1 and Equation 3.2 (Table 4.1). Then, the corrosion rate of aluminium alloys is calculated by using Equation 3.3 in unit of µg /h /cm^2 and plotted in Figure 4.1.

Table 4.1: Average weight loss and corrosion rate of the samples.

Biodiesel Blend	Aluminium Alloy	Average Weight Loss, $W_{loss,avg}$ (mg)	Corrosion Rate (µg /h /cm^2)
B0	AA 3003	1.2778	0.0628
	AA 5052	0.6667	0.0327
	AA 6061	0.8667	0.0426
B5	AA 3003	1.4889	0.0731
	AA 5052	1.2000	0.0589
	AA 6061	1.2667	0.0622
B10	AA 3003	1.8000	0.0884
	AA 5052	1.4889	0.0731
	AA 6061	1.6556	0.0813
B15	AA 3003	2.1778	0.1070
	AA 5052	1.8444	0.0906
	AA 6061	2.0222	0.0993

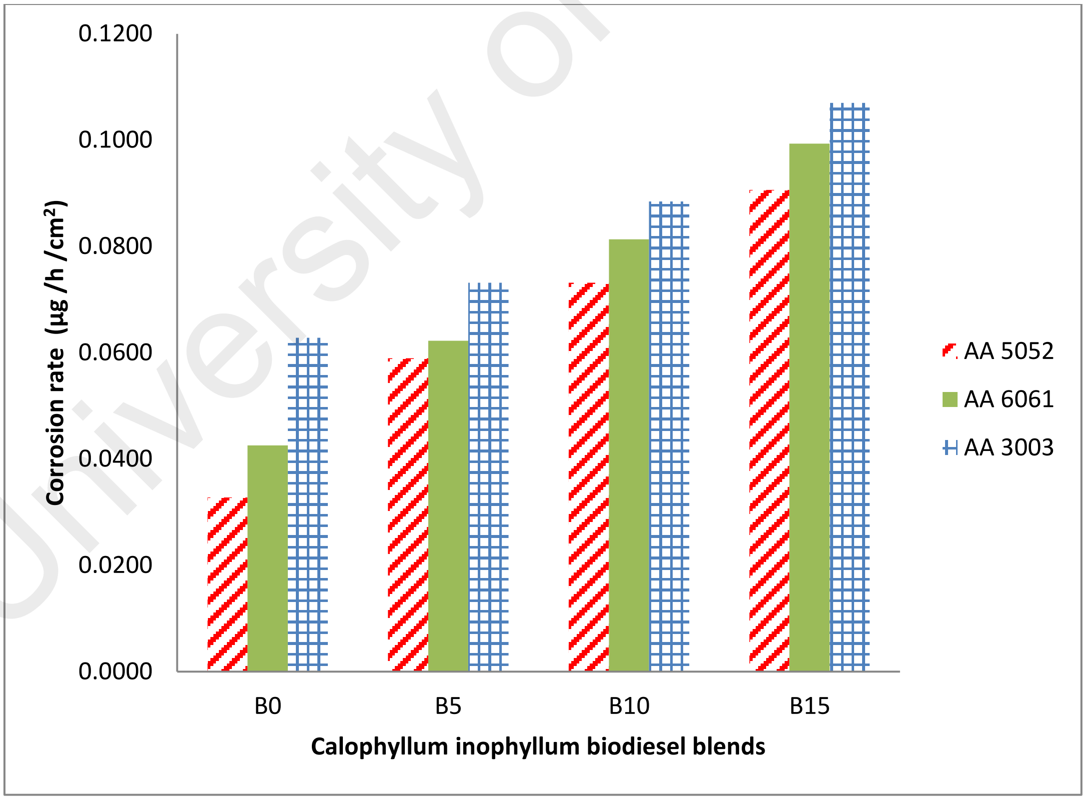

Figure 4.1 : Corrosion rate of aluminium alloys after immersion in Calophyllum inophyllum biodiesel blends at room temperature for 1200h.

From this study, the lowest corrosion rate for each aluminium alloy sample is observed in Calophyllum inophyllum biodiesel blend B0 while the highest corrosion rate is observed in B15. The corrosion rate of aluminium alloy 3003 in B0, B5, B10 and B15 is 0.0628 µg /h /cm^2, 0.0731 µg /h /cm^2, 0.0884 µg /h /cm^2 and 0.1070 µg /h /cm^2 respectively. The corrosion rate of aluminium alloy 5052 in B0, B5, B10 and B15 is 0.0327 µg /h /cm^2, 0.0589 µg /h /cm^2, 0.0731 µg /h /cm^2 and 0.0906 µg /h /cm^2 respectively. The corrosion rate of aluminium alloy 6061 in B0, B5, B10 and B15 is 0.0426 µg /h /cm^2, 0.0622 µg /h /cm^2, 0.0813 µg /h /cm^2 and 0.0993 µg /h /cm^2. From the data, the corrosion rate of aluminium alloy 3003, 5052 and 6061 increases as the content of Calophyllum inophyllum biodiesel in blend increases.

This shows that more aluminium alloy atom dissolute as the concentration of unsaturated fatty acid chain increases in higher Calophyllum inophyllum biodiesel blends. Higher Calophyllum inophyllum biodiesel blend contain more fatty acid chain that is more prone to oxidation that can cause the biodiesel blends become more corrosive. As the oxidation stability reduces in high Calophyllum inophyllum biodiesel content, fatty acid in the higher biodiesel blend are more susceptible to oxidation, thus more oxidation reactions occur in high biodiesel blend. From the oxidation, more acid produced in high biodiesel blend, hence more aluminium alloy atom dissolute in the high biodiesel blend. The dissolution of aluminium atom results reduces the weight of the aluminium alloy sample and corrodes the surface of the aluminium alloy samples.

Compared to the other studies, Fazal et al. show that the biodiesel is more corrosive then petroleum diesel by comparing the corrosion rate between diesel and pure palm biodiesel (Fazal et al., 2010). Norouzi et al. also reported that increase of the content of rapeseed methyl ester biodiesel increases the corrosion rate of aluminium and copper

(Norouzi, Eslami, Wyszynski, & Tsolakis, 2012). Another study done by Su et al also shows that corrosion rate increases as the content of rapeseed biodiesel increases in biodiesel blend (Su et al., 2014). The same corrosion behavior is also observed from a study done by Cursaru et al. when the aluminium, copper and mild carbon steel is allowed to immersed in sunflower biodiesel blends B0, B20 and B100 (Cursaru, Brănoiu, Ramadan, & Miculescu, 2014). This concludes that the high content of biodiesel in biodiesel blend is more corrosive compared to diesel.

The corrosion in Calophyllum inophyllum biodiesel can be reduced by improving the oxidation stability of biodiesel. The oxidation stability of biodiesel can be increased by adding more amount of petroleum diesel so that the number of unsaturated fatty acid can be reduced for the same volume used. The addition of palm oil can also improve the oxidation stability of biodiesel. A study done by R. Sarin et. al and show that the oxidation stability of Jatropha curcas improves when blended with palm biodiesel (R. Sarin, Sharma, Sinharay, & Malhotra, 2007). Besides, the oxidation stability of soybeen oil and rapessed oil is also improved when blended with palm oil from a study done by Park et. al (Park et al., 2008). Both R. Sarin et al. and Park et. al conclude that high content of saturated fatty acid in palm oil improves the oxidation stability in biodiesel blends.

The corrosion rate of the three samples is different in Calophyllum inphyllum biodiesel blend B0, B5, B10 and B15. In B0, the corrosion rate of aluminium alloy 3003, 6061 and 5052 is 0.0628 µg /h /cm^2, 0.0426 µg /h /cm^2 and 0.0327 µg /h /cm^2 respectively. In B5, the corrosion rate of aluminium alloy 3003, 6061 and 5052 is 0.0731 µg /h /cm^2, 0.0622 µg /h /cm^2 and 0.0589 µg /h /cm^2 respectively. In B10, the corrosion rate of aluminium alloy 3003, 6061 and 5052 is 0.0884 µg /h /cm^2, 0.0813 µg /h /cm^2 and 0.0731 µg /h /cm^2 respectively. In B15, the corrosion rate of aluminium alloy 3003, 6061 and 5052 is 0.1070 µg /h /cm^2, 0.0993 µg /h /cm^2 and 0.0906 µg /h /cm^2 respectively. The result shows that the aluminium alloy 3003 has the highest corrosion rate, followed by aluminium alloy 6061 while aluminium alloy 5052 has the lowest corrosion rate for all Calopyllum inophyllum biodiesel B0, B5, B10 and B15 blends.

The result shows that different aluminium alloy has different corrosion resistant to Calophyllum inophyllum biodiesel blends. Different chemical composition in aluminium alloy 3003, 6061 and 5052 affects the corrosion rate in Calophyllum inophyllum biodiesel blends. Magnesium and manganese content in the alloy affects the corrosion rate of aluminium alloys in Calophyllum inophyllum biodiesel blends. Based on the result, aluminium alloy 5052, which contain the highest magnesium, has the lowest corrosion rate while aluminium alloy 3003, which contain the highest manganese has the highest corrosion rate. High magnesium content provides more passive area in the alloy since both aluminium and magnesium produce passive layer aluminium oxide, Al_2O_3 and magnesium oxide, MgO on the alloy surface, hence increases the corrosion resistance (Perez et al., 2017). Due to the potential difference between magnesium and aluminium, the magnesium reacts as anode while aluminium reacts as cathode, thus affecting the stability of the protection layer. High manganese content increases the corrosion rate of aluminium alloy. The corrosion rate increases as the manganese content increases might due to the production of Mn-enriched second phase in aluminium alloy 3003 if the content of manganese exceed 1.25% in alloy (Y. Liu & Cheng, 2010). The addition of excess manganese creates galvanic potential between Mn-enriched second phase and Al-matrix where the Mn-enriched second phase become cathode and Al-matrix becomes anode, hence breaks the oxide layer film, thus the pitting corrosion initiate at Al-matrix. Aluminium alloy 6061 has moderate corrosion resistance due to its magnesium and silicon principle alloying element. Since both aluminium alloy 5052 and 6061 contain magnesium, the corrosion resistance in these alloys are greater than aluminium alloy 3003. But, the corrosion rate of aluminium alloy 6061 is greater than 5052 due to the presence of silicon and higher iron content. The Al-Fe-Si intermetallic increase the cathodic reaction, hence increase the dissolution of Al-matrix that act as anode during the reaction (Mutombo, 2011). Besides, low copper and iron content in aluminium alloy 5052 reduces the corrosion rate in Calophyllum inophyllum biodiesel blends. Low content of copper and iron reduces the Al_2Cu and Al_3Fe intermetallic density, hence reduces the cathodic reaction in intermetallic, thus reduces the susceptibility to the pitting corrosion in Al-matrix (Birbilis & Buchheit, 2005).

Compared to another corrosion study of aluminium alloys, Kishan Roodbari reported that the aluminium alloy 5052 has the lowest corrosion rate, followed by aluminium alloy 6061 and 6063 while aluminium alloy 3003 has the highest corrosion rate when exposed to NaCl solution (Kishan Roodbari, 2015). In another study done by Wang et al., Al-Mg alloy has better corrosion resistance and passivation behavior compared to Al-Mn alloy when exposed to 3.5% NaCl aqueous solution (Wang et al., 2016). These studies show that Al-Mg alloy has better corrosion resistance compared to Al-Mn. Between aluminium alloy 5xxx series and 6xxx series, Birol et al. found out that the weight loss of 5xxx series is lower than 6xxx series when immersed in 3.5% NaCl for 472 days (Birol & Birol, 2004).

4.3 Surface Characterization

4.3.1 Sample Before Immersion Test

Figure 4.2 and Figure 4.3 (enlarged view) show the image of aluminium alloys 3003, 5052 and 6061 before the immersion test. Aluminium alloys 3003, 5052 and 6061 are grinded using grit paper grade 600, 800 and 1200 and observed using SEM. BSE image of these samples are used as reference and compared to the image after immersion.

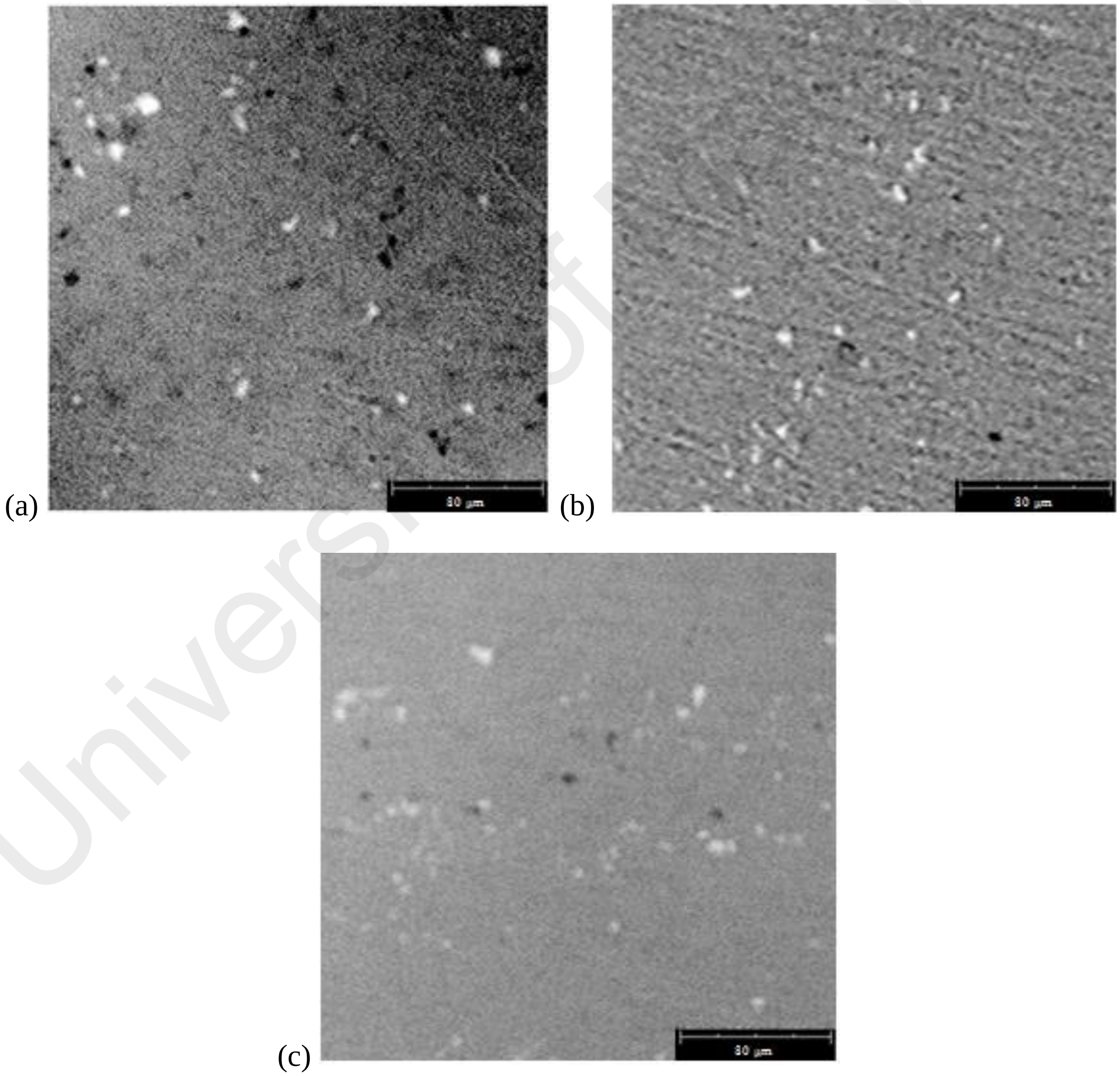

Figure 4.2: BSE-SEM image before immersion test at 1000X

(a) AA 3003, (b) AA 5052, and (c) AA 6061

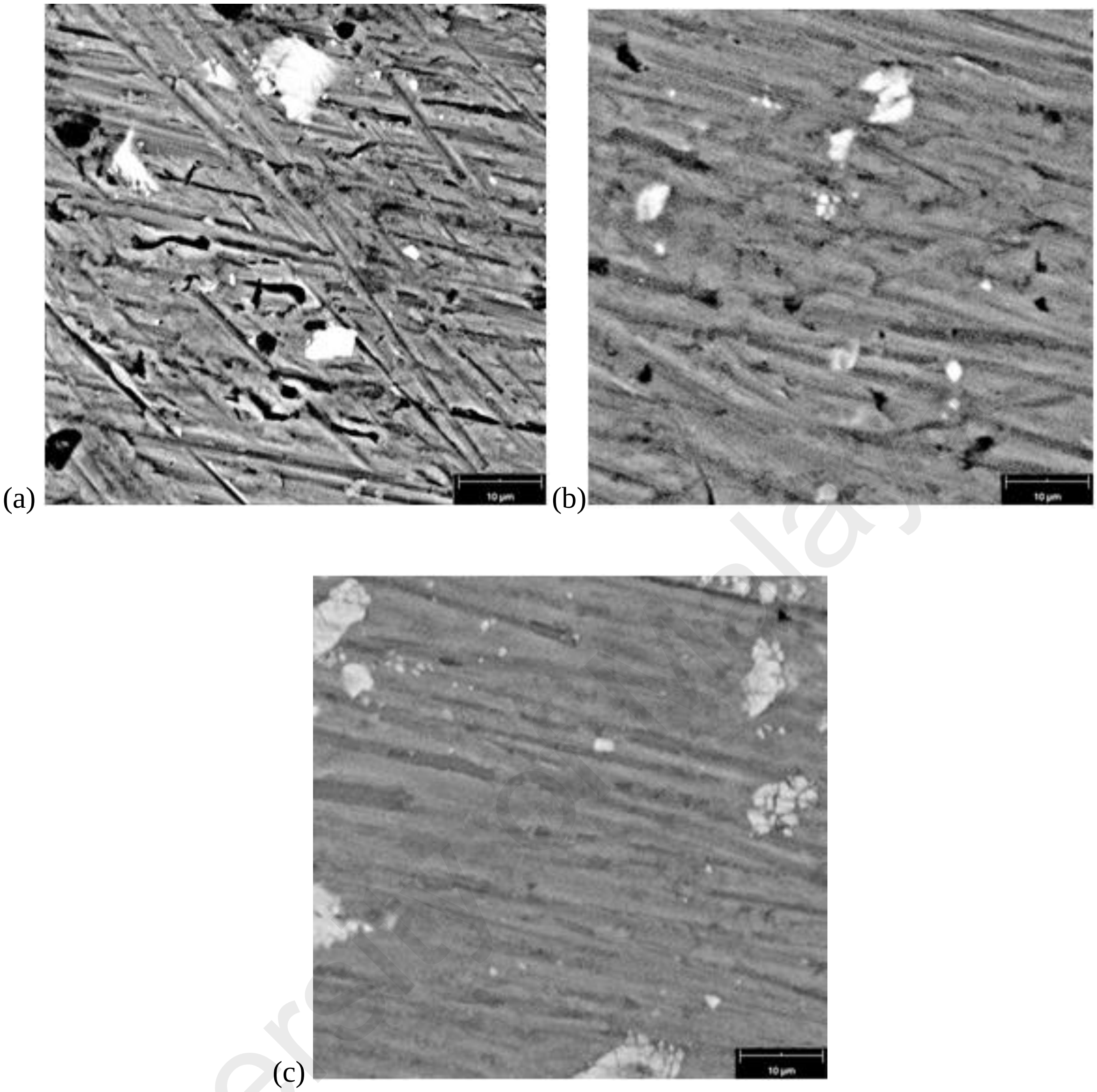

Figure 4.3: BSE-SEM image before immersion test at 4500X

(a) AA 3003, (b) AA 5052, and (c) AA 6061

4.3.2 Immersion in B0

Figure 4.4 and Figure 4.5 (enlarged view) show the surface of aluminium alloys 3003, 5052 and 6061 after immersed in B0 for 1200 hours at room temperature. A few pits are observed on the surface of aluminium alloy 3003 (Figure 4.4(a)), while no pitting observed on the surface of aluminium alloy 5052 and 6061 (Figure 4.4(b) & Figure 4.4(c)).

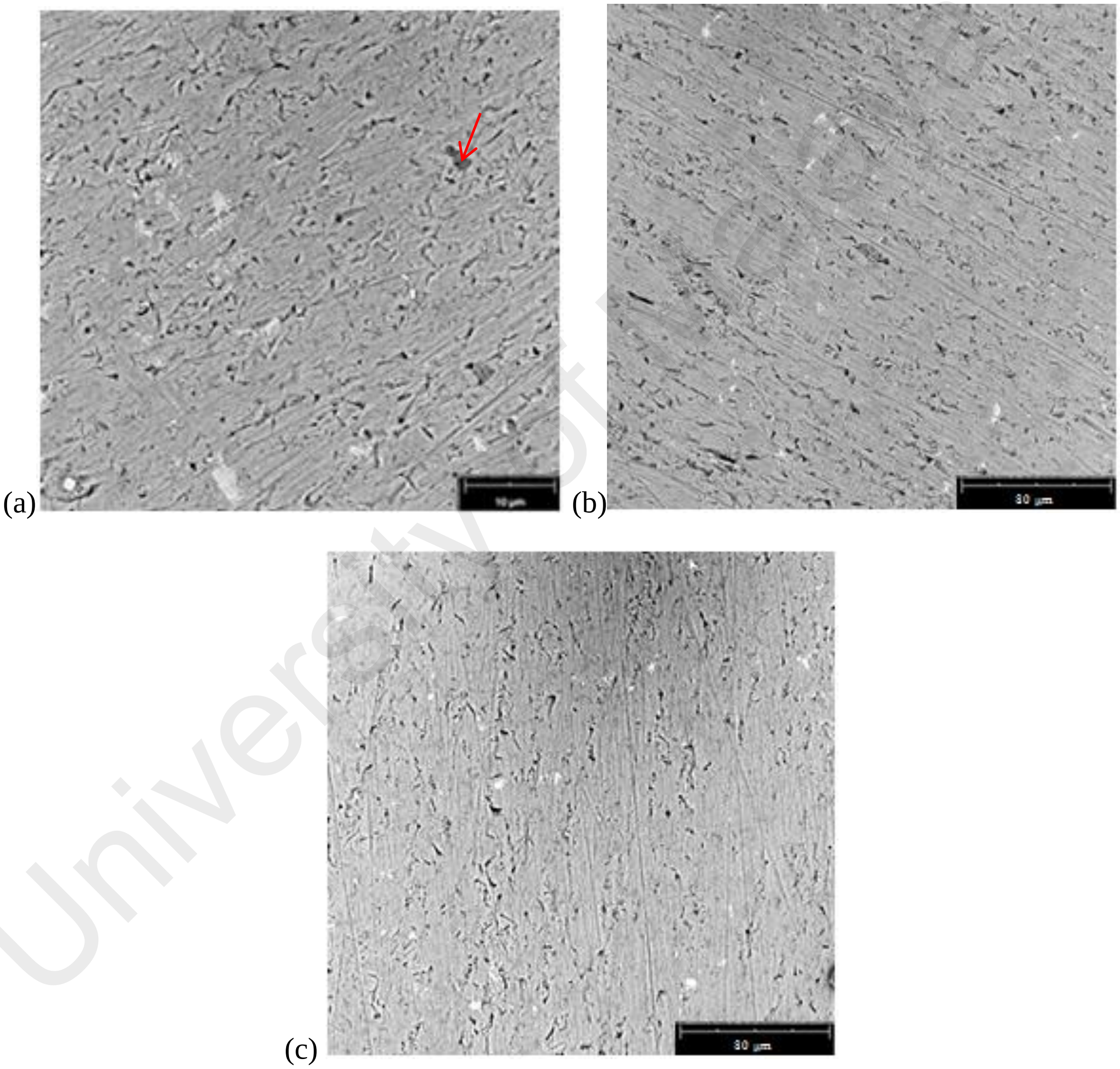

Figure 4.4: BSE-SEM image after immersion test in B0 at 1000X

(a) AA 3003, (b) AA 5052, and (c) AA 6061

Figure 4.5(a) shows the wide circular pitting formation on the surface of aluminium alloy 3003. While there is no pitting formed on the surface of aluminium alloys 5052 and 6061 (Figure 4.5(b) & Figure 4.5(c)). Result shows that aluminium alloy 3003 is susceptible to pitting attacks when immersed in B0. Since there is no pitting on the surface of aluminium alloys 5052 and 6061, the atoms in these aluminium alloys probably dissolute uniformly in commercial biodiesel.

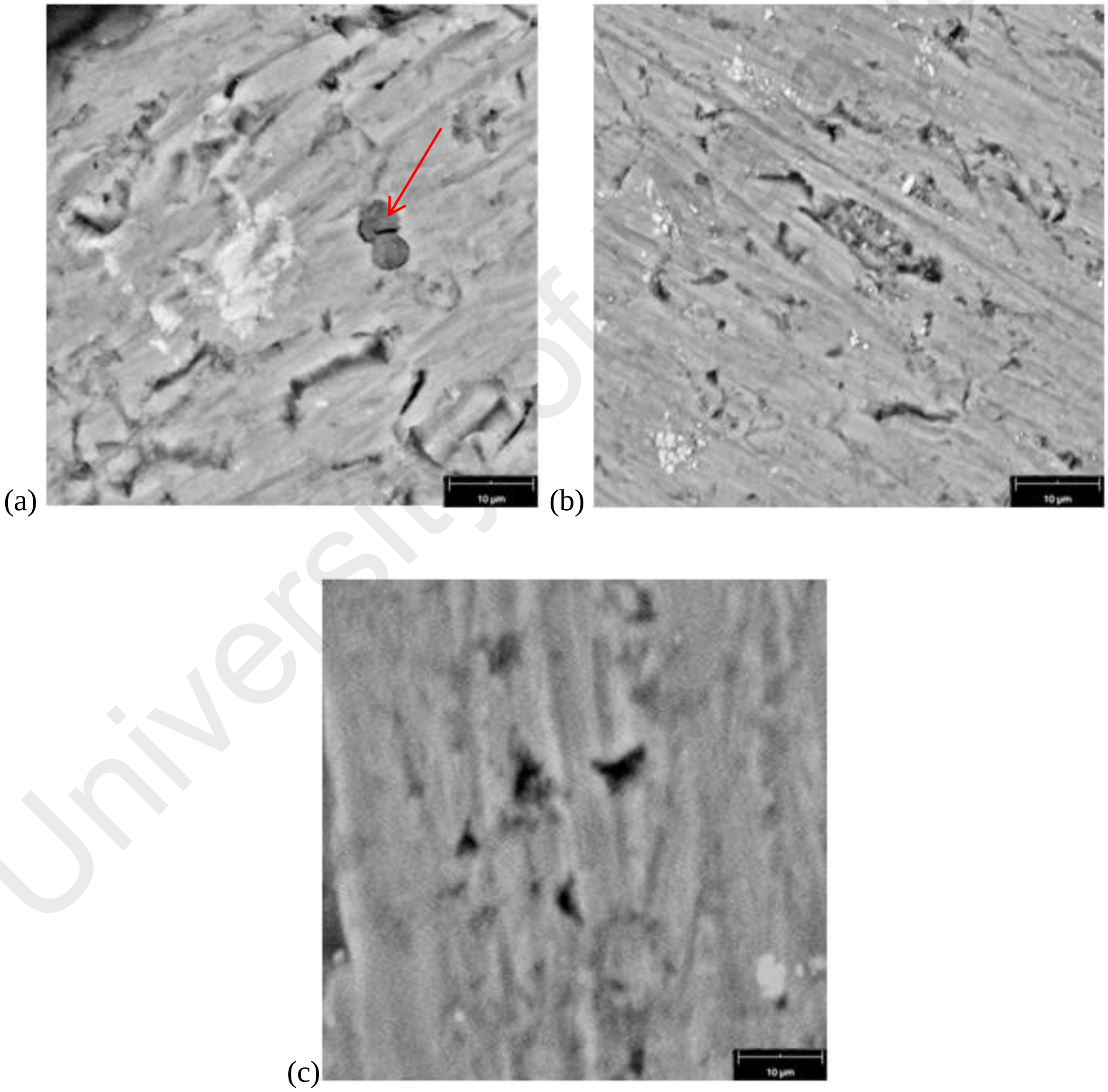

Figure 4.5: BSE-SEM image after immersion test in B0 at 4500X

(a) AA 3003, (b) AA 5052, and (c) AA 6061

4.3.3 Immersion in Calophyllum Inophyllum Biodiesel Blend B15

Figure 4.6 and Figure 4.7 (enlarged view) show the image of surface of aluminium alloys of 3003, 5052 and 6061 after immersed in Calophyllum inophyllum biodiesel B15 blend for 1200 hours at room temperature. A few pits are observed on the surface of aluminium alloy 3003 (Figure 4.6(a)), while there is no pitting on the surface of aluminium alloy 5052 and 6061 (Figure 4.6(b) & Figure 4.6(c)).

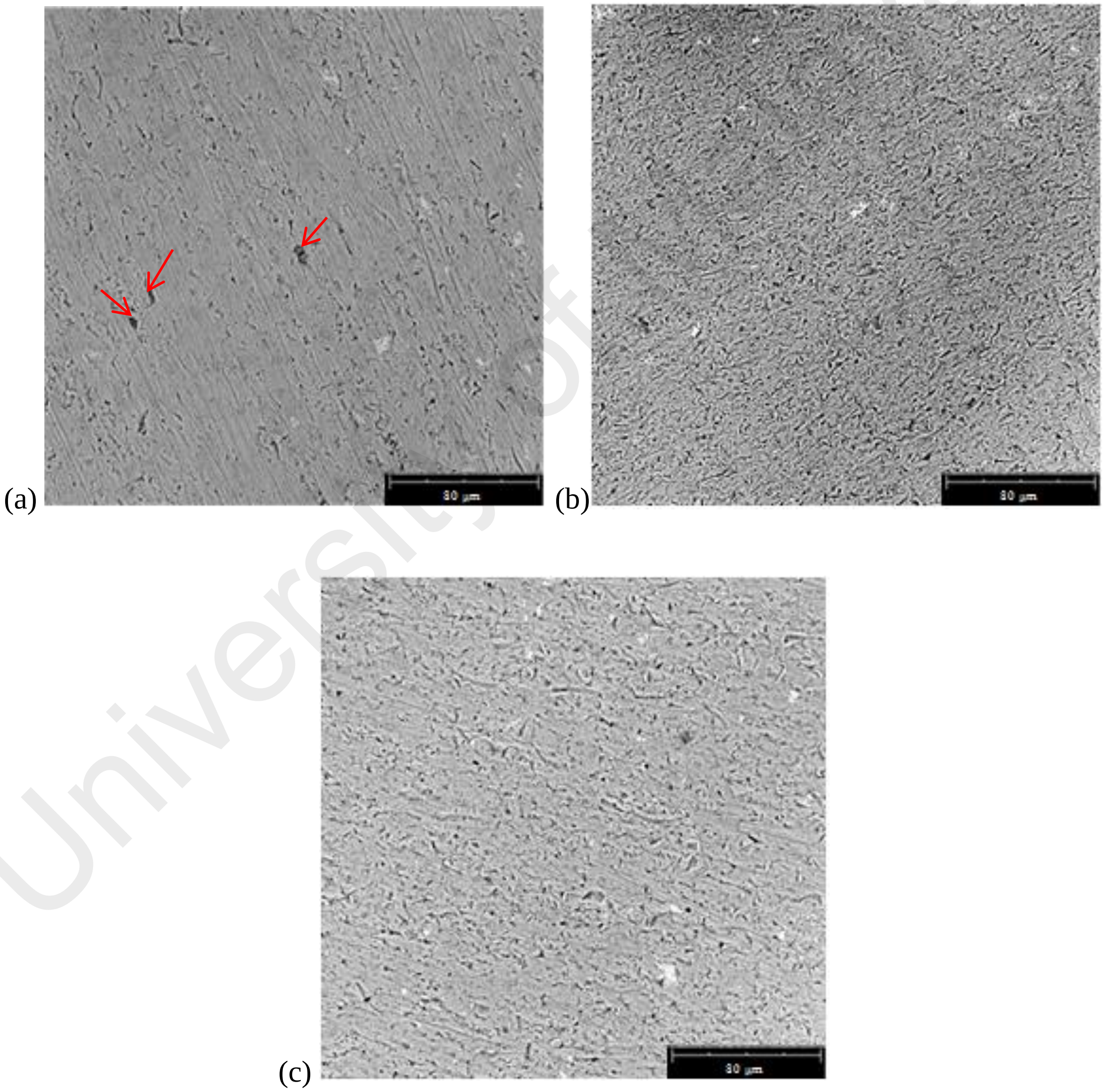

Figure 4.6: BSE-SEM image after immersion test in B15 at 1000X

(a) AA 3003, (b) AA 5052, and (c) AA 6061

Figure 4.7 (a) shows the oval shaped pitting formation on the surface of aluminium alloy 3003. While there is no pitting formed on the surface of aluminium alloys 5052 and 6061 (Figure 4.7(b) & Figure 4.7(c)). From the observation, aluminium alloy 3003 is prone to pitting attacks while aluminium alloys 5052 and 6061 is most probably corrode uniformly when immersed in Calophyllum inophyllum biodiesel blends.

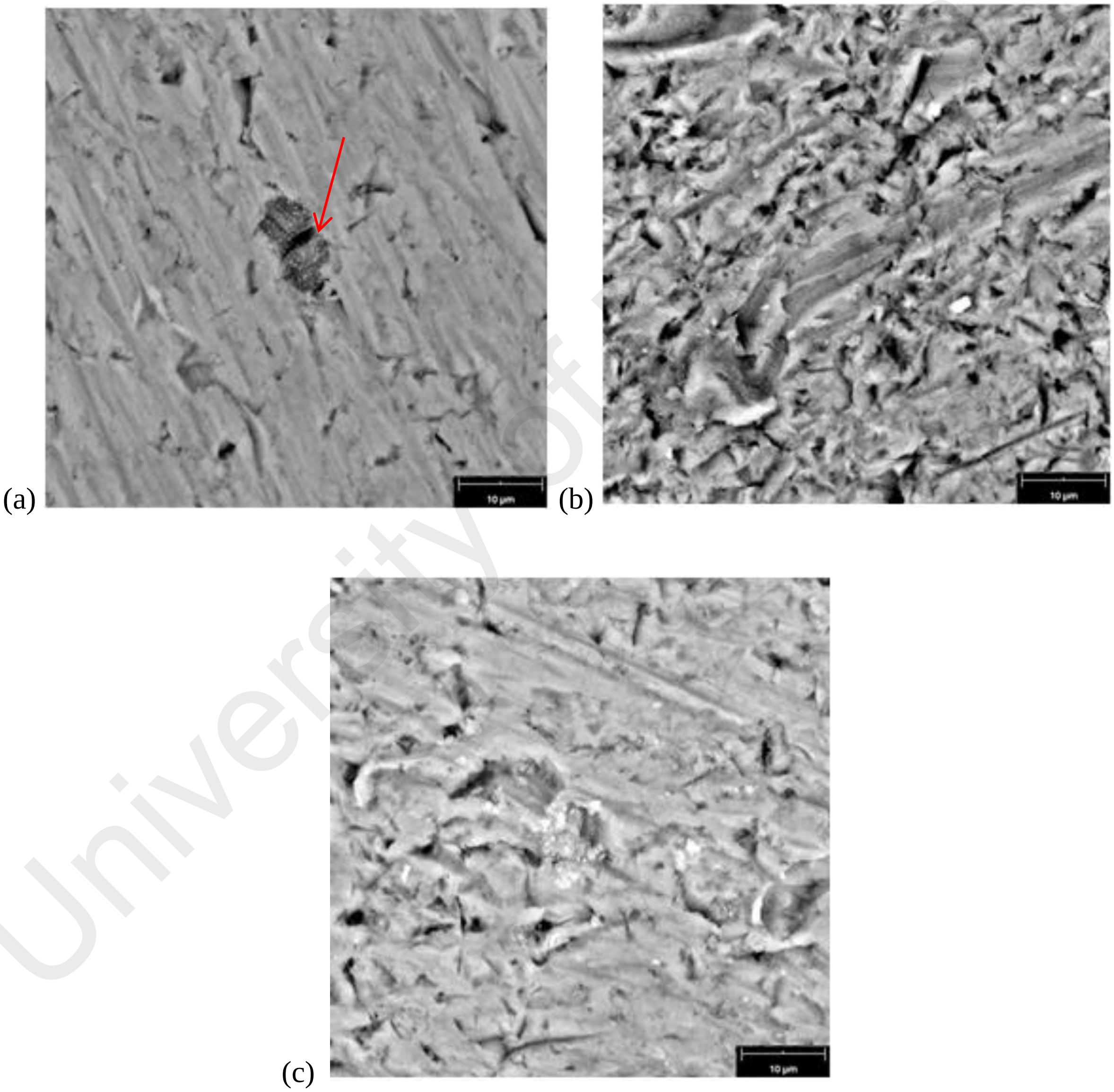

Figure 4.7: BSE-SEM image after immersion test in B15 at 4500X

(a) AA 3003, (b) AA 5052, and (c) AA 6061

From the result, aluminium alloy 3003 is prone to pitting corrosion, while aluminium alloy 5052 and 6061 is suspected to have uniform corrosion when immersed in Calophyllum inophyllum biodiesel blends. The presence of manganese disrupts the protective oxide layer formed by aluminium in aluminium alloy 3003, hence shorten the passive region (Kishan Roodbari, 2015). The spots that are not protected by oxide layer exposed its bare surface to Calophyllum inophyllum biodiesel blends, thus the electrochemical reaction occur in that region. The surface that exposed directly to the Calophyllum inophyllum biodiesel blends acts as anode while the surface covered by oxide layer act as cathode. As a result, atoms at anode dissolute and initiate pitting formation on the surface of aluminium alloy 3003.

For aluminium alloy 3003, it is observed that more pitting formed on the surface when immersed in Calophyllum inophyllum biodiesel B15 blend compared to B0. As the content of Calophyllum inophyllum biodiesel increases, the pitting corrosion on the surface of aluminium 3003 becomes more severe. High content of unsaturated fatty acid in high Calophyllum inophyllum biodiesel blends enhance the corrosion process, thus initiate more pitting on the surface of aluminium alloy 3003. This shows that the Calophyllum inophyllum biodiesel is more corrosive compared to commercial biodiesel. Fazal et al. found out that the pitting density formed on the aluminium in palm biodiesel is higher compared to petroleum diesel due to the high concentration of oxygen in palm biodiesel (Fazal et al., 2010). Norouzi et al. also observed that the pitting become more severe as the content of rapeseed methyl ester increases in biodiesel blend (Norouzi et al., 2012).

In both aluminium alloy 5052 and 6061, the corrosion process in Calophyllum inophyllum biodiesel blends is suspected to occur in uniform manner. The formation of protective film on the surface of aluminium alloy 5052 and 6061 is more even compared to aluminium alloy 3003 due to the magnesium presence in aluminium alloy 5052 and 6061 (Perez et al., 2017). Since the protective film covers all surfaces, there is no region that exposed directly to Calophyllum inophyllum biodiesel blends, hence there will be no pitting formation on the surface.

CHAPTER 5: CONCLUSION

In this work, the corrosion behavior of three aluminiums alloys 3003, 5052 and 6061 in Calophyllum inophyllum biodiesel blends for 1200 hours at room temperature is studied by using immersion test and SEM characterization. A few conclusions from this study are stated as follow.

- The corrosion behavior of aluminium alloy in Calophyllum inophyllum biodiesel blend is dependent on the chemical composition in the aluminium alloy. Aluminium alloy 3003 has a consistent highest corrosion rate in Calophyllum inophyllum biodiesel blends B0, B5, B10 and B15 due to the highest manganese content in its alloy compared to aluminium alloy 5052 and 6061. Aluminium alloy 5052 has a consistent lowest corrosion rate in Calophyllum inophyllum biodiesel blends B0, B5, B10 and B15 due to the highest magnesium content in its alloy compared to aluminium alloy 3003 and 6061.
- The blending percentage of Calophyllum inophyllum biodiesel blends affects the corrosion behavior of aluminium alloy 3003, 5052 and 6061. Increasing in Calophyllum inophyllum biodiesel content in biodiesel blend increases the corrosion rate of aluminium alloy 3003, 5052 and 6061. The highest weight loss is observed in Calophyllum inophyllum biodiesel blend B15, while the lowest weight loss is observed in commercial biodiesel B0 for aluminium alloy 3003, 5052 and 6061 after immersion test for 1200 hours at room temperature.
- Surface morphology from the corrosion process of the aluminium alloy in Calophyllum inophyllum biodiesel blends is highly related to the chemical composition of the aluminium alloys. Aluminium alloy 3003 is susceptible to

pitting corrosion, while there are no pits observed in aluminium alloy 5052 and 6061 immersed in Calophyllum inophyllum biodiesel blends for 1200 hours at room temperature. The pitting forms on the surface of aluminium alloy 3003 due to its high manganese content that disrupt the passive layer on its surface. Aluminium alloy 5052 and 6061 has high magnesium content in its alloy that provide continuous protective layer on its surface, hence prevent the pitting formation on its surface.

In future, the corrosion study of Calophyllum inophyllum biodiesel can be done at different temperature. Diesel engine has average operating temperature around 90 ^{o}C, so it is better to study the corrosion behavior at working temperature to simulate the corrosion activity during the operation of diesel engine. The temperature may affect the corrosion rate of Calophyllum inophyllum biodiesel since the kinetic energy of molecules is different at different temperature, so the study on the effect of temperature on corrosion behavior of Calophyllum inophyllum biodiesel may provide the vital information towards the application of Calophyllum inophyllum biodiesel in future.

REFERENCE

Agoramoorthy, G., Sarnaik, J., Mungikar, R., Punde, S., & Hsu, M. J. (2012). Non-edible oil seed producing Calophyllum inophyllum ideal for India's future biofuel development. *Gcb Bioenergy, 4*(6), 708-712.

Ahmad, Z. (2006). *Principles of corrosion engineering and corrosion control*: Butterworth-Heinemann.

Alenezi, R., Baig, M., Wang, J., Santos, R., & Leeke, G. (2010). Continuous flow hydrolysis of sunflower oil for biodiesel. *Energy Sources, Part A: Recovery, Utilization, and Environmental Effects, 32*(5), 460-468.

Antolın, G., Tinaut, F., Briceno, Y., Castano, V., Perez, C., & Ramırez, A. (2002). Optimisation of biodiesel production by sunflower oil transesterification. *Bioresource technology, 83*(2), 111-114.

Armbruster, W., & Coyle, W. (2006). Pacific food system outlook 2006–2007: the future role of biofuels. Pacific Economic Cooperation Council, Singapore.

Ashok, B., Nanthagopal, K., & Vignesh, D. S. (2017). Calophyllum inophyllum methyl ester biodiesel blend as an alternate fuel for diesel engine applications. *Alexandria Engineering Journal*.

Association, A. (2009). International alloy designations and chemical composition limits for wrought aluminum and wrought aluminum alloys. *Arlington, VA: The Aluminum Association*.

Association, E. A. (2002). The aluminium automotive manual. *EAA*.

Atabani, A., & da Silva César, A. (2014). Calophyllum inophyllum L.–A prospective non-edible biodiesel feedstock. Study of biodiesel production, properties, fatty acid composition, blending and engine performance. *Renewable and Sustainable Energy Reviews, 37*, 644-655.

Atabani, A., Mahlia, T., Masjuki, H., Badruddin, I. A., Yussof, H. W., Chong, W., & Lee, K. T. (2013). A comparative evaluation of physical and chemical properties of biodiesel synthesized from edible and non-edible oils and study on the effect of biodiesel blending. *Energy, 58*, 296-304.

Baboian, R. (1995). Corrosion Test and Standards Manual. *ASTM Manual Series, Fredericksburg*, 149.

Banga, S., & Varshney, P. K. (2010). Effect of impurities on performance of biodiesel: A review. *Journal of Scientific & Industrial Research, 69*, 575-579.

Birbilis, N., & Buchheit, R. (2005). Electrochemical characteristics of intermetallic phases in aluminum alloys an experimental survey and discussion. *Journal of the Electrochemical Society, 152*(4), B140-B151.

Birol, F., & Birol, Y. (2004). *Corrosion behavior of twin-roll cast al-mg and al-mg-si alloys.* Paper presented at the Proceedings of the 9th International Conference on Aluminium Alloys.

Chisti, Y. (2007). Biodiesel from microalgae. *Biotechnology advances, 25*(3), 294-306.

Cursaru, D.-L., Brănoiu, G., Ramadan, I., & Miculescu, F. (2014). Degradation of automotive materials upon exposure to sunflower biodiesel. *Industrial Crops and Products, 54*, 149-158.

Davis, J. (1994). Aluminium and aluminium alloy. *ASM Speciality Handbook (ASM International, USA, 1994).*

Davis, J. R. (1999). *Corrosion of aluminum and aluminum alloys*: Asm International.

Davis, J. R. (2001). *Alloying: understanding the basics*: ASM international.

Downs, A. J. (1993). *Chemistry of aluminium, gallium, indium and thallium*: Springer Science & Business Media.

Dudley, B. (2016). BP Statistical Review of World Energy June 2016 (65 ed.). US: bp.

Dudley, B. (2017). BP statistical review of world energy. June 2012. *London, UK*.

Fattah, I. R., Masjuki, H., Kalam, M., Wakil, M., Ashraful, A., & Shahir, S. A. (2014). Experimental investigation of performance and regulated emissions of a diesel engine with Calophyllum inophyllum biodiesel blends accompanied by oxidation inhibitors. *Energy conversion and management, 83*, 232-240.

Fazal, M., Haseeb, A., & Masjuki, H. (2010). Comparative corrosive characteristics of petroleum diesel and palm biodiesel for automotive materials. *Fuel Processing Technology, 91*(10), 1308-1315.

Foidl, N., Foidl, G., Sanchez, M., Mittelbach, M., & Hackel, S. (1996). Jatropha curcas L. as a source for the production of biofuel in Nicaragua. *Bioresource technology, 58*(1), 77-82.

Friday, J., & Okano, D. (2006). Calophyllum inophyllum (kamani). *Species profiles for Pacific Island agroforestry, 2*(1), 1-17.

Ghadge, S. V., & Raheman, H. (2005). Biodiesel production from mahua (Madhuca indica) oil having high free fatty acids. *Biomass and Bioenergy, 28*(6), 601-605.

Haseeb, A., Masjuki, H., Ann, L., & Fazal, M. (2010). Corrosion characteristics of copper and leaded bronze in palm biodiesel. *Fuel Processing Technology, 91*(3), 329-334.

Haseeb, A., Sia, S., Fazal, M., & Masjuki, H. (2010). Effect of temperature on tribological properties of palm biodiesel. *Energy, 35*(3), 1460-1464.

Hu, E., Xu, Y., Hu, X., Pan, L., & Jiang, S. (2012). Corrosion behaviors of metals in biodiesel from rapeseed oil and methanol. *Renewable energy, 37*(1), 371-378.

Jahirul, M. I., Koh, W., Brown, R. J., Senadeera, W., O'Hara, I., & Moghaddam, L. (2014). Biodiesel production from non-edible beauty leaf (Calophyllum inophyllum) oil: Process optimization using response surface methodology (RSM). *Energies, 7*(8), 5317-5331.

Jin, D., Zhou, X., Wu, P., Jiang, L., & Ge, H. (2015). Corrosion behavior of ASTM 1045 mild steel in palm biodiesel. *Renewable energy, 81*, 457-463.

Kafuku, G., & Mbarawa, M. (2010). Biodiesel production from Croton megalocarpus oil and its process optimization. *Fuel, 89*(9), 2556-2560.

Kaul, S., Saxena, R., Kumar, A., Negi, M., Bhatnagar, A., Goyal, H., & Gupta, A. (2007). Corrosion behavior of biodiesel from seed oils of Indian origin on diesel engine parts. *Fuel Processing Technology, 88*(3), 303-307.

Kaya, C., Hamamci, C., Baysal, A., Akba, O., Erdogan, S., & Saydut, A. (2009). Methyl ester of peanut (Arachis hypogea L.) seed oil as a potential feedstock for biodiesel production. *Renewable energy, 34*(5), 1257-1260.

Kelly, R. G., Scully, J. R., Shoesmith, D., & Buchheit, R. G. (2002). *Electrochemical techniques in corrosion science and engineering*: CRC Press.

Kishan Roodbari, M. (2015). *Effect of Microstructure on the Performance of Corrosion Resistant Alloys.* NTNU.

Koh, H. L. (2009). *A guide to medicinal plants: an illustrated, scientific and medicinal approach*: World Scientific.

Liu, X., He, H., Wang, Y., Zhu, S., & Piao, X. (2008). Transesterification of soybean oil to biodiesel using CaO as a solid base catalyst. *Fuel, 87*(2), 216-221.

Liu, Y., & Cheng, Y. (2010). Role of second phase particles in pitting corrosion of 3003 Al alloy in NaCl solution. *Materials and corrosion, 61*(3), 211-217.

Ma, F.-Y. (2012). Corrosive effects of chlorides on metals *Pitting Corrosion*: InTech.

Ma, F., & Hanna, M. A. (1999). Biodiesel production: a review. *Bioresource technology, 70*(1), 1-15.

Mahmudul, H., Hagos, F., Mamat, R., Adam, A. A., Ishak, W., & Alenezi, R. (2017). Production, characterization and performance of biodiesel as an alternative fuel in diesel engines–A review. *Renewable and Sustainable Energy Reviews, 72*, 497-509.

Mattos, R. A. d., Bastos, F. A., & Tubino, M. (2015). Correlation Between the Composition and Flash Point of Diesel-Biodiesel Blends. *Journal of the Brazilian Chemical Society, 26*(2), 393-395.

McNaught, A., & Wilkinson, A. (2012). IUPAC. Compendium of Chemical Terminology, (the" Gold Book"): redox potential. 2012.

Metals, A. C. G.-o. C. o. (2011). *Standard practice for preparing, cleaning, and evaluating corrosion test specimens*: ASTM International.

Miller, W., Zhuang, L., Bottema, J., Wittebrood, A. J., De Smet, P., Haszler, A., & Vieregge, A. (2000). Recent development in aluminium alloys for the automotive industry. *Materials Science and Engineering: A, 280*(1), 37-49.

Mofijur, M., Rasul, M., Hyde, J., Azad, A., Mamat, R., & Bhuiya, M. (2016). Role of biofuel and their binary (diesel–biodiesel) and ternary (ethanol–biodiesel–diesel) blends on internal combustion engines emission reduction. *Renewable and Sustainable Energy Reviews, 53*, 265-278.

Moore, C. (2005). National transportation statistics. *Bureau of Transportation Statistic, US Department of Transportation, Washington DC, 20590*.

Murray, D. (2005). Ethanol's potential: looking beyond corn. Earth Policy Institute.

Mutombo, K. (2011). *Intermetallic particles-induced pitting corrosion in 6061-T651 aluminium alloy.* Paper presented at the Materials science forum.

Naik, M., Meher, L., Naik, S., & Das, L. (2008). Production of biodiesel from high free fatty acid Karanja (Pongamia pinnata) oil. *Biomass and Bioenergy, 32*(4), 354-357.

Nakpong, P., & Wootthikanokkhan, S. (2010). High free fatty acid coconut oil as a potential feedstock for biodiesel production in Thailand. *Renewable energy, 35*(8), 1682-1687.

Nelson, L. S., Shih, R. D., Balick, M. J., & Lampe, K. F. (2007). *Handbook of poisonous and injurious plants*: Springer.

Nitske, W. R., & Wilson, C. M. (1965). *Rudolph Diesel: pioneer of the age of power*: University of Oklahoma Press.

Norouzi, S., Eslami, F., Wyszynski, M. L., & Tsolakis, A. (2012). Corrosion effects of RME in blends with ULSD on aluminium and copper. *Fuel Processing Technology, 104*, 204-210.

OECD, & FAO. (2009). Agricultural Outlook 2009 - 2018. London: Organisation for Economic Cooperation and Development (OECD) and Food and Agriculture Organization (FAO).

Ong, H., Mahlia, T., Masjuki, H., & Norhasyima, R. (2011). Comparison of palm oil, Jatropha curcas and Calophyllum inophyllum for biodiesel: a review. *Renewable and Sustainable Energy Reviews*, *15*(8), 3501-3515.

Ostermann, F., & Woodward, R. (1993). Aluminum materials technology for automobile construction. *London Mechanical Engineering Publications Limited, 1*.

Owen, N. A., Inderwildi, O. R., & King, D. A. (2010). The status of conventional world oil reserves—Hype or cause for concern? *Energy policy, 38*(8), 4743-4749.

Park, J.-Y., Kim, D.-K., Lee, J.-P., Park, S.-C., Kim, Y.-J., & Lee, J.-S. (2008). Blending effects of biodiesels on oxidation stability and low temperature flow properties. *Bioresource technology, 99*(5), 1196-1203.

Pereira, M. C., Silva, J. W., Acciari, H. A., Codaro, E. N., & Hein, L. R. (2012). Morphology characterization and kinetics evaluation of pitting corrosion of commercially pure aluminium by digital image analysis. *Materials Sciences and Applications, 3*(05), 287.

Perez, O., Valdez, S., Molina, A., Mejia-Sintillo, S., Garcia-Perez, C., Salinas-Bravo, V., & Gonzalez-Rodriguez, J. (2017). Corrosion Behavior of Al–Mg–Zn-Si Alloy Matrix Composites Reinforced with Y_2O_3 in 3.5% NaCl Solution. *Int. J. Electrochem. Sci, 12*, 7300-7311.

Pleanjai, S., & Gheewala, S. H. (2009). Full chain energy analysis of biodiesel production from palm oil in Thailand. *Applied energy, 86*, S209-S214.

Pullen, J., & Saeed, K. (2012). An overview of biodiesel oxidation stability. *Renewable and Sustainable Energy Reviews, 16*(8), 5924-5950.

Ramadhas, A. S., Jayaraj, S., & Muraleedharan, C. (2005). Biodiesel production from high FFA rubber seed oil. *Fuel, 84*(4), 335-340.

Rashid, U., & Anwar, F. (2008). Production of biodiesel through optimized alkaline-catalyzed transesterification of rapeseed oil. *Fuel, 87*(3), 265-273.

Revie, R. W. (2008). *Corrosion and corrosion control*: John Wiley & Sons.

Rosegrant, M. W. (2008). *Biofuels and grain prices: impacts and policy responses*: International Food Policy Research Institute Washington, DC.

Sanchez, F., & Vasudevan, P. T. (2006). Enzyme catalyzed production of biodiesel from olive oil. *Applied biochemistry and biotechnology, 135*(1), 1-14.

Sarin, A. (2012). *Biodiesel: production and properties*: Royal Society of Chemistry.

Sarin, R., Sharma, M., Sinharay, S., & Malhotra, R. K. (2007). Jatropha–palm biodiesel blends: an optimum mix for Asia. *Fuel, 86*(10), 1365-1371.

Singh, B., Korstad, J., & Sharma, Y. (2012). A critical review on corrosion of compression ignition (CI) engine parts by biodiesel and biodiesel blends and its inhibition. *Renewable and Sustainable Energy Reviews, 16*(5), 3401-3408.

Soltis, J. (2015). Passivity breakdown, pit initiation and propagation of pits in metallic materials–review. *Corrosion Science, 90*, 5-22.

Su, Y., Chen, F., Wu, Z., & Wang, H. (2014). *Corrosion characteristics of biodiesel in storage.* Paper presented at the Materials for Renewable Energy and Environment (ICMREE), 2013 International Conference on.

Sudradjat, R. (2011). Calophyllum inophyllum L. a potential plant for biodiesel.

Szklarska-Smialowska, Z. (1999). Pitting corrosion of aluminum. *Corrosion Science, 41*(9), 1743-1767.

Szklarska-Smialowska, Z., & ZS-Smialowska. (2005). *Pitting and crevice corrosion*: NACE International Houston, TX.

Testing, A. S. f., & Materials. (2010). *Standard Specification for Diesel Fuel Oils*.

Thangavelu, S. K., Ahmed, A. S., & Ani, F. N. (2016). Impact of metals on corrosive behavior of biodiesel–diesel–ethanol (BDE) alternative fuel. *Renewable energy, 94*, 1-9.

Van Gerpen, J. (1996). *Cetane number testing of biodiesel.* Paper presented at the Proceedings of the third liquid fuels conference.

Venkanna, B., & Reddy, C. V. (2009). Biodiesel production and optimization from Calophyllum inophyllum linn oil (honne oil)–A three stage method. *Bioresource technology, 100*(21), 5122-5125.

Wang, B., Liu, J., Yin, M., Xiao, Y., Wang, X., & He, J. (2016). Comparison of corrosion behavior of Al-Mn and Al-Mg alloys in chloride aqueous solution. *Materials and corrosion, 67*(1), 51-59.

Yaakob, Z., Narayanan, B. N., & Padikkaparambil, S. (2014). A review on the oxidation stability of biodiesel. *Renewable and Sustainable Energy Reviews, 35*, 136-153.

Zaid, B., Saidi, D., Benzaid, A., & Hadji, S. (2008). Effects of pH and chloride concentration on pitting corrosion of AA6061 aluminum alloy. *Corrosion Science, 50*(7), 1841-1847.

Ziółkowska, M., & Wardzińska, D. (2015). Corrosiveness of Fuels During Storage Processes *Storage Stability of Fuels*: InTech.

Zuleta, E. C., Baena, L., Rios, L. A., & Calderón, J. A. (2012). The oxidative stability of biodiesel and its impact on the deterioration of metallic and polymeric materials: a review. *Journal of the Brazilian Chemical Society*, *23*(12), 2159-2175.